MTL TR 87-35

ERRORS ASSOCIATED WITH FLEXURE TESTING OF BRITTLE MATERIALS

FRANCIS I. BARATTA and WILLIAM T. MATTHEWS
MECHANICS AND STRUCTURES DIVISION

GEORGE D. QUINN
CERAMICS RESEARCH DIVISION

July 1987

US ARMY
LABORATORY COMMAND
MATERIALS TECHNOLOGY
LABORATORY

U.S. ARMY MATERIALS TECHNOLOGY LABORATORY
Watertown, Massachusetts 02172-0001

The findings in this report are not to be construed as an official Department of the Army position, unless so designated by other authorized documents.

Mention of any trade names or manufacturers in this report shall not be construed as advertising nor as an official indorsement or approval of such products or companies by the United States Government.

DISPOSITION INSTRUCTIONS

Destroy this report when it is no longer needed.
Do not return it to the originator.

REPORT DOCUMENTATION PAGE

READ INSTRUCTIONS BEFORE COMPLETING FORM

1. REPORT NUMBER: MTL TR 87-35	2. GOVT ACCESSION NO.
3. RECIPIENT'S CATALOG NUMBER	
4. TITLE (and Subtitle): ERRORS ASSOCIATED WITH FLEXURE TESTING OF BRITTLE MATERIALS	5. TYPE OF REPORT & PERIOD COVERED: Final Report
6. PERFORMING ORG. REPORT NUMBER	
7. AUTHOR(s): Francis I. Baratta, George D. Quinn, and William T. Matthews	8. CONTRACT OR GRANT NUMBER(s)
9. PERFORMING ORGANIZATION NAME AND ADDRESS: U.S. Army Materials Technology Laboratory, Watertown, Massachusetts 02172-0001, SLCMT-MSR	10. PROGRAM ELEMENT, PROJECT, TASK AREA & WORK UNIT NUMBERS
11. CONTROLLING OFFICE NAME AND ADDRESS: U.S. Army Laboratory Command, 2800 Powder Mill Road, Adelphi, Maryland 20783-1145	12. REPORT DATE: July 1987
	13. NUMBER OF PAGES: 49
14. MONITORING AGENCY NAME & ADDRESS (if different from Controlling Office)	15. SECURITY CLASS. (of this report): Unclassified
	15a. DECLASSIFICATION/DOWNGRADING SCHEDULE

16. DISTRIBUTION STATEMENT (of this Report)

Approved for public release; distribution unlimited.

17. DISTRIBUTION STATEMENT (of the abstract entered in Block 20, if different from Report)

18. SUPPLEMENTARY NOTES

This report is a revised, corrected, and expanded form of AMMRC TR 82-20.

19. KEY WORDS (Continue on reverse side if necessary and identify by block number)

Flexural strength
Ceramic materials
Mechanical properties
Error analysis

20. ABSTRACT (Continue on reverse side if necessary and identify by block number)

DD FORM 1 JAN 73 1473 EDITION OF 1 NOV 65 IS OBSOLETE

Block No. 20

ABSTRACT

Requirements for accurate bend-testing of four-point and three-point beams of rectangular cross-section are outlined. The so-called simple beam theory assumptions are examined to yield beam geometry ratios that will result in minimum error when utilizing elasticity theory. Factors that give rise to additional errors when determining bend strength are examined, such as: wedging stress, contact stress, load mislocation, beam twisting, friction at beam contact points, contact point tangency shift, and neglect of corner radii or chamfer in the stress determination. Also included are the appropriate Weibull strength relationships and an estimate of errors in the determination of the Weibull parameters based on sample size. Such analyses and results provide guidance for the accurate determination of flexure strength of brittle materials within the linear elastic regime. Error tables resulting from these analyses are presented.

CONTENTS

NOMENCLATURE

E	Young's modulus of the test material
E_c	Young's modulus in compression of the test material
E_T	Young's modulus in tension of the test material
F	The probability of failure of a component
G	Shear modulus of the beam material
I	Moment of inertia for a rectangular beam ($I = bd^3/12$)
$(I_{xx})_c$	Moment of inertia for a rectangular beam with 45^o chamfered corners (See Appendix F)
$(I_{xx})_r$	Moment of inertia for a rectangular beam with round corners (See Appendix F)
L	Outer span length for a four-point and a three-point loaded beam
L_T	Total length of beam
M	Weibull slope parameter, the "Weibull Modulus" associated with either volume or surface sensitive material
M_b	General moment applied to beam
M_x	Bending moment as a function of x (See Appendix D or E)
P	General applied force
P_1, P_2, P_3, P_4	Forces applied to a beam (See Figure 1)
S_e	Effective surface of a beam in bending
T_b	Torque associated with beam twisting
T_{b_e}	Estimated torque when bottoming of the load fixture occurs (See Appendix C)
V	Volume of a beam in bending
V_e	Effective volume of a beam in bending (See Weibull Analysis)
V_L	Volume of a three-point loaded beam ($V_L = Lbd$) in the risk of rupture equation
a	Half the distance between the inner span and outer span for a four-point loaded beam, i.e., $(L-\ell)/2$ or $a=L/2$ for a three-point loaded beam (note $a_1 = a_2 = a$)
a_1 and a_2	A beam dimension (See Figures 1 and 2)
b	Beam width (See Figure 1 or 5)
c	Chamfer of a corner of a beam with 45^o chamfers (See Figure 5)
d	Beam depth (See Figure 1 or 5)
e	Load eccentricity equal to (a_1-a)
e/L	Load eccentricity ratio equal to $(a_1-a)/L$
e_c	Shift of neutral axis in an initially curved beam

e_m	Error in the specimen diemnsions b or d
e_s	Error in the span lengths ℓ or L
h_1, h_2	Horizontal shift of contact and load points due to beam bending (See Figure 4)
k_1, k_2	A numerical factor dependent upon b/d (See Appendix C)
ℓ	Inner span length of a four-point loaded beam (See Figure 1)
ℓ'	Either equal to "a" or L/2 for four-point or three-point beam systems
n	Numerical factor (See Equation 18b)
p_{max}	Maximum contact pressure at the load application point
r	Radius of the corners of the beam (See Figure 5)
s	Speed of loading
t	Time of loading
x_1, x_2, x_3	Variable beam distances (See Figure 1c)
x'	Variable distance (failure site location) on either side of the load contact point (See Appendix D)
x,y	Coordinate axes (See Figure 1)
y	Can also be displacement or distance from neutral axis as defined in the text
α_b, α_c	Beam curvature parameters (See Equations 3a and 4a)
β	Anticlastic curvature factor (See Appendix A)
β_T	A numerical factor associated with the tensile stress caused by load contact (See Appendix D)
γ	$\gamma = \sqrt[4]{3(1-\nu^2)/d^2\rho^2}$ (See Appendix A)
$\varepsilon_x, \varepsilon_y, \varepsilon_z$	Strain in the x, y, and z directions
$\dot{\varepsilon}$	Strain rate
$\bar{\varepsilon}$	Percent error, defined as $[(\sigma_b - \sigma_x)/\sigma_x]100$. A negative error indicates the simple beam equations 1a and 1b underestimate the true stress; a positive error is an overestimate.
θ	Angle of a plane inclined to x-axis
θ^*	Angle of a plane inclined to the x-axis at which the principal stress is maximum
μ	Coefficient of friction
ν	Poisson's ratio
ρ	Radius of curvature of a beam due to bending
ρ_1	Contact radius of a support point (See Figure 4)
ρ_2	Contact radius of a load point (See Figure 4)
ρ_c	Initial radius of the curvature of a beam
σ_b	Bending stress in a beam as defined by simple beam theory or mean fracture stress

σ_n	Normal stress (See Appendix C)
$\sigma_{n_{max}}$	Maximum principal stress (See Appendix C)
σ_o	Scale parameter or characteristic value associated with a Weibull analysis
σ_x	Stress in the x direction (along the beam length)
σ_z	Stress in the z direction (along the beam width)
τ_{xy}	Shear stress due to torsion (See Appendix C)
ϕ_s	Angle of twist along the specimen length (See Figure 3 and Appendix C) in Radians
ϕ_F	Angle of twist between a pair of load and contact points (See Figure 3 and Appendix C) in Radians

INTRODUCTION

There has been an increase in interest and activity in recent years in both the research and development of ceramic materials and their practical application to engineering structures.

Flexural testing is (and will likely remain) the primary source of uniaxial strength data, either for quality control or design data purposes. An impediment to the use of flexural strength data in either application is the lack of standard test methods and the presence of experimental error in current practices.

In 1973, a tentative unapproved set of standards* was prepared by the Army Materials and Mechanics Research Center (AMMRC) as it was called at that time, and distributed to interested and involved organizations. This set of unofficial standards, which included such test methods as flexure, tension, creep, stress rupture, fatigue, and spin testing, was discussed at several meetings of government and industry representatives. A number of worthwhile suggestions evolved. However, it was apparent that these tentative standards were inadequate and thus not approved. Recently, however, interest was revived at AMMRC, now called the U.S. Army Materials Technology Laboratory (MTL), in finalizing standard tests for brittle materials. It was viewed that the original tentative standards, dated 2 April 1973, represented the ideal goal but were far too inclusive to realistically establish testing requirements which would provide valid results at this time. It was decided to concentrate upon developing a standard method for flexural strength testing.

The objective of this report is to recommend beam test systems such that accurate fracture strength measurements will result when testing brittle materials within the elastic regime. This report differs from Reference 1 in the following ways:

1. Discussions of a "Reference Standard" beam system have been deleted in deference to a different approach adopted in Reference 2.

2. The error table for nonlinear stress has been eliminated because it was redundant with errors analyzed from "wedging stresses."

3. The twisting error analysis has been reanalyzed as a plane stress condition.

4. Additional analyses, refinements, and corrections to the original work have been included where appropriate.

No attempt has been made to determine the influence of each error upon the total error of the system. It is assumed that each error is independent of all the other error sources. Thus, for consistency and simplicity, the total error within the system is assumed to be the sum of the parts. Errors in flexure testing of beams are either due to assumptions entailed in simple beam theory, or to sources arising from external load applications. The sources of error are discussed in the following sections.

*Military Standards, Test Methods for Structural Ceramics, 2 April 1973.

1. BARATTA, F. I. *Requirements for Flexure Testing of Brittle Materials*. U. S. Army Materials and Mechanics Research Center, AMMRC TR 82-20, April 1982, ADA 113937.
2. U. S. ARMY MIL-STD-1942 (MR). *Flexure Testing of High Performance Ceramics at Ambient Temperature*. November 1983.

ERRORS FROM SIMPLE BEAM THEORY ASSUMPTIONS

The rectangular beam configuration is attractive as a strength-test vehicle because of its simple shape and apparent ease of load application, as well as analysis and reduction of data. Rods of circular cross section are also used in beam tests, but usually for specialized testing. Because a beam of circular cross section is not as frequently used as the rectangular beam, only the rectangular cross section is examined in the discussions to follow. Referring to Figures 1a and 2a for dimensions and applied loads, the simple beam formulas for maximum stress in flexure are:

$$\sigma_b = 3P(L-\ell)/2bd^2 \qquad \text{for a four-point beam} \qquad (1a)$$

$$\sigma_b = 3PL/2bd^2 \qquad \text{for a three-point beam} \qquad (1b)$$

A critical review of simple beam theory assumptions will yield ranges of geometry ratios by which the theory can be validly applied. These assumptions are listed below, as well as their associated inferences in terms of an error analysis:

1. Transverse planes perpendicular to the longitudinal axis of the beam remain plane after the beam is deflected.

2. The modulus of elasticity in tension is equal to the modulus of elasticity in compression. Also, the beam material is isotropic and homogeneous.

3. The maximum deflection must be small compared to the beam depth.

4. The beam must deflect normally under elastic bending stresses but not through any local collapse or twisting.

5. Stresses in the longitudinal direction are independent of lateral displacements.

Each of the above assumptions is examined in detail, where possible, so that the required rectangular beam geometry ratios can be determined as a function of the associated errors.

Assumptions 1 and 2 together imply that stress and strain are proportional to the distance from the neutral axis, and the stress does not exceed the proportional limit of the material. These assumptions disregard the effect of any shearing resistance and make impossible the use of the flexure formula for curved beams of large curvature.

Assumption 1 and the above implication suggest that the bending stress is proportional to the distance from the neutral axis to the outer surface of the beam. This assumption is valid if flexure of the beam could be attained without applying local forces to the beam. However, practical flexure test systems, such as those shown in Figures 1a and 2a, which utilize four-point and three-point beams, require direct contact of the fixture to the specimen to apply loads and thus moments to the specimens. At the point of contact there will be compressive stress in the beam depth direction resulting in a local variation from linearity in the bending stress.[3]

3. TIMOSHENKO, S., and GOODIER, J. N. *Theory of Elasticity*. 2nd Ed., McGraw-Hill Book Co., Inc., New York, 1951.

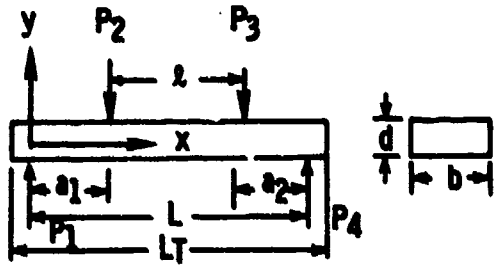

(a) Idealized Loading $a_1 = a_2 = a$

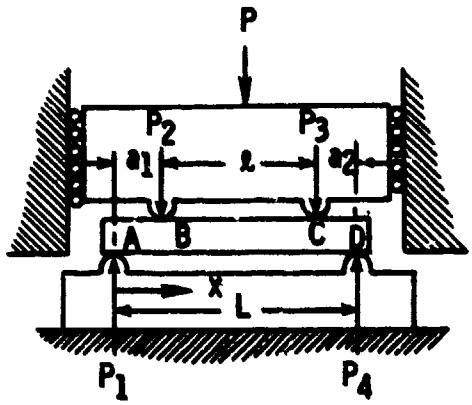

(b) Nonpivoting Rigid Loading Head $a_1 \neq a_2$

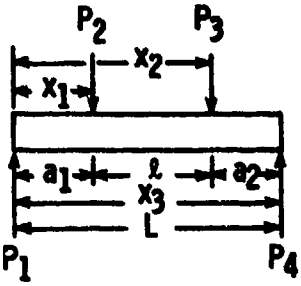

(c) Loading when $x_1 \neq x_3 = x_2$

Figure 1. Four-point loading.

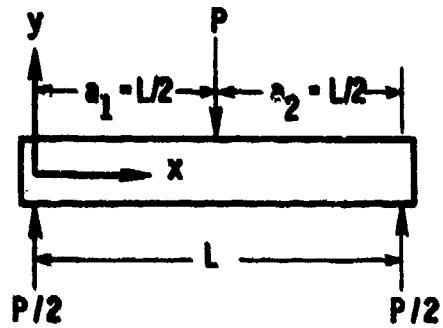

(a) Idealized Loading

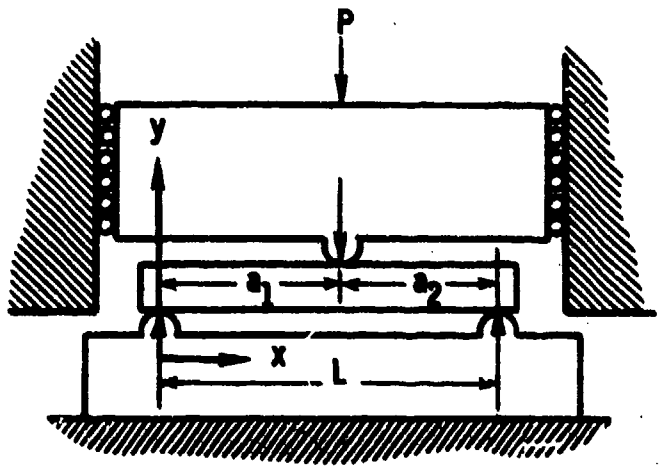

(b) Nonpivoting Rigid Loading Head; $a_1 \neq a_2 \neq L/2$

Figure 2. Three-point loading.

Because this contribution to bending stress nonlinearity, referred to as wedging stress,[4] is caused by external load application, it will be discussed further in detail under the section entitled Errors From External Influences.

An error source that is internal to the beam arises because of the assumption that the modulus of elasticity in tension is equal to that in compression, $E_T = E_c$. Chamlis[5] has derived in closed form the solution for the tensile bending stress when $E_T \neq E_c$. After some manipulation of the appropriate formulas,[5] the tensile stress due to bending is given by:

$$\sigma_x = (\sigma_b/2)[1 + (E_T/E_c)^{1/2}], \tag{2}$$

for both the four-point and the three-point loaded beams. The resulting percent error is given in Table 1.

Table 1. ERROR WHEN $E_T \neq E_c$

E_T/E_c	% Error	E_T/E_c	% Error
0.20	+38.2	1.025	-0.6
0.40	+22.5	1.050	-1.2
0.60	+12.7	1.075	-1.8
0.80	+5.6	1.10	-2.4
0.90	+2.6	1.15	-3.5
0.925	+1.9	1.20	-4.6
0.950	+1.3	1.30	-6.5
0.975	+0.6	1.40	-8.4
1.00	0	1.60	-11.7
		1.80	-14.6
		2.0	-17.2

Although the errors associated with neglecting to account for anisotropy and nonhomogeneity of the test material are not considered here, they are briefly mentioned in the following paragraphs so that the reader will be aware of such possibilities.

If the beam is anisotropic, the bending stress formula is exactly the same as the elementary theory except that the application of a bending moment can produce twisting moment. According to Lekhnitskii,[6] determining the accompanying shear stress produced by bending a rod of rectangular cross section, having only one plane of elastic symmetry normal to the axis, is very complicated. (Composite and crystal structures are excluded here as test materials.) If the degree of anisotropy for ceramic material is slight, it may be permissible to assume that the error when ignoring this effect on the fracture stress will also be small.

Nonhomogeneity of the test material infers variation of the elastic modulus. It has been observed* that in plates of hot-pressed silicon nitride, the modulus of elasticity at the surface is several percent different than that of the center. This

*Private discussion with E. M. Lenoe, MTL.

4. TIMOSHENKO, S. *Strength of Materials.* 3rd Ed., D. Van Nostrand Co., Inc., N.Y., 1958, and Part II, 2nd Ed., D. Van Nostrand Co., Inc., N.Y. 1941.
5. CHAMLIS, C. C. *Analysis of Three-Point-Bend Test for Materials with Unequal Tension and Compressive Properties.* NASA TN D7572, March 1974.
6. LEKHNITSKII, S. G. *Theory of Elasticity of an Anisotropic Elastic Body.* Holden-Day Series in Mathematical Physics, J. L. Brandstatter, ed., 1963, p. 204.

is also an area in which further analysis will be required to assess the error applicable to four-point and three-point loaded beams when the modulus of elasticity varies through the beam thickness.

If a rectangular beam has initial curvature ρ_c, the error can be determined from an analysis provided by Timoshenko.[4] The general bending stress σ_x in a curved beam due to a pure moment is given by the following:

$$\sigma_x = \alpha_c(M_b/bd\rho_c) \tag{3}$$

where

$$\alpha_c = \frac{(d/2\rho_c) - (e_c/\rho_c)}{(e_c/\rho_c)[1 - (d/2\rho_c)]} \tag{3a}$$

$$e_c/\rho_c = [(d/\rho_c)^2/12][1 + (d/\rho_c)^2/15]. \tag{3b}$$

Since the bending stress, according to simple beam theory, is $\sigma_b = 6M_b/bd^2$, and putting σ_b in the same terms as (3) above, we have:

$$\sigma_b = \alpha_b(M_b/bd\rho_c), \tag{4}$$

where

$$\alpha_b = 6(\rho_c/d). \tag{4a}$$

The percent error $\bar{\varepsilon}$ for a beam of rectangular cross section and of beam-to-depth initial curvature ρ_c/d resulting in a neutral axis shift of e_c/ρ_c is:

$$\bar{\varepsilon} = 100[(\alpha_b - \alpha_c)/\alpha_c]. \tag{5}$$

The resulting error for a beam of rectangular cross section bent by a pure moment as obtained from (5) is given in Table 2 as a function of initial curvature. It is assumed that an analogous analysis applied to a three-point loaded beam would produce similar results.

The validity of the assumption that the strain is proportional to the distance from the neutral axis and that stresses are independent of lateral displacements is dependent upon the ratio of the beam width to its depth. Anticlastic curvature of rectangular beams or plates with intermediate ratios of b/d can lead to erroneous results using simple beam theory; see Timoshenko.[7] Of course, if the beam can be considered infinite in width, like a plate, the correction of the bending stress is simply[8] $1/(1 - \nu^2)$. The question arises as to what ratios of b/d are appropriate for the application of simple beam theory. Ashwell[9] examined in detail the anticlastic curvature of rectangular beams and plates and provided the answer to this

7. TIMOSHENKO, S. *Letter to the Editor.* Mechanical Engineering, v. 45, no. 4, April 1923, p. 259-260.
8. BARATTA, F. I. *When is a Beam a Plate?* J. Amer. Cer. Soc., v. 64, no. 5, 1981, p. c-86.
9. ASHWELL, D. G. *The Anticlastic Curvature of Rectangular Beams and Plates.* J. Roy., Aero. Soc., v. 54, 1950, p. 708-715.

question. The pertinent formulas taken from Reference 9 are given in Appendix A. These equations were applied to ceramic materials with Poisson's ratio ν equal to 0.25 and the ratio of Young's modulus to fracture stress E/σ_b of 1000 to determine the percent error* using simple beam theory as a function of b/d which is shown in Table 3.

Table 2. ERROR CAUSED BY INITIAL BEAM CURVATURE

ρ_c/d	% Error
1	35.1
2	16.7
3	10.9
4	8.4
10	3.2
15	2.2
20	1.7
40	0.8
100	0.3

$\varepsilon = 100\ [(\alpha_b - \alpha_c)/\alpha_c]$

Note: All errors are negative.

Table 3. ERROR CAUSED BY EFFECT OF ANTICLASTIC CURVATURE

$E/\sigma_b = 1 \times 10^3$

b/d	% Error
1.0	0
15.0	0
20.0	0.1
30.0	0.6
40.0	1.5
50.0	2.6
100.0	4.7
500.0	5.9
1000.0	6.1
∞	$\rightarrow (-\nu^2)100 = -6.25\%$

Note: All errors are negative.

If the maximum deflection is not small compared to the beam depth, linear beam theory cannot be employed without an error. West[10] examined large deflections of three-point loaded beams, and from such results a definitive ratio of beam length-to-depth can be determined for valid application of simple beam formulas. Since for most brittle materials values of E/σ_b range from approximately 500 to 1000, the former value was used to compute the percent error because it would yield the largest error. Although the analysis was applied to a three-point loaded beam, the method was extended to determine errors for four-point loaded beams as well. The results of the calculations using the mentioned analysis[10] are presented in Table 4, which gives errors for four-point and three-point loaded beams as a function of L/d.

Table 4. ERROR FOR BEAMS WITH LARGE DEFLECTION

$E/\sigma_b = 500$

L/d	Four-Point	Three-Point
0	0	0
25	0.1	0.1
50	0.6	0.4
100	1.4	1.0
150	2.5	1.8
200	4.1	2.9
250	7.0	4.9

Note: All errors are negative.

*Ashwell considered a beam bent by a constant moment analogous to the four-point beam loading case, which should represent a conservative bound on b/d for the three-point beam, as well.

10. WEST, D. C. *Flexure Testing of Plastics.* Exp. Mech., v. 21, no. 2, July 1964.

It is implicit in the assumptions given in Reference 10 that the loads and moments are applied to the beam in an ideal manner with no friction occurring between the load application points and the beam. Ritter and Wilson[11] have determined a beam length-to-depth limit based on the minimization of friction effects when large deflections occur. The friction effect considered is that which gives rise to a moment caused by the slope at the load application point. Not considered in the analysis[11] are the effects of friction due to a moment acting out of the neutral plane of the beam, lateral contraction or extension, and changes in moment arms due to contact point tangency shift. These factors will be discussed later.

Returning to the results of Reference 11, an inequality for the four-point-loaded beam which provides a limit is given in the following:

$$(L/d - a/d)/(E/\sigma_b) \leq 0.3 \tag{6}$$

to insure negligible nonlinear deflections and friction effects. The value of 0.3 was obtained from limiting the slope to less than 15° between the beam in the loaded and unloaded positions at the outermost support point. If the minimum value of E/σ_b is chosen to be 500, then we determine that for a four-point loaded beam (6) becomes:

$$L/d - a/d \leq 150. \tag{7}$$

It is noted from Table 4 that neglecting beam deflections resulted in greater error in calculation of bending stress for the four-point loaded beam than for the three-point loaded beam. For conservatism, therefore, it will be assumed that (7) is applicable to the three-point loaded beam as well, with $a/d = 0$. Thus (7) becomes

$$L/d \leq 150. \tag{8}$$

It appears that these limits are compatible with those values given in Table 4 such that reasonable L/d ratios can be chosen that will result in small errors when minimizing deflection.

One of the last requirements, no buckling of the beam, is easily fulfilled for ceramic materials with beam dimensions of practical test configurations. The reader can readily verify this statement by referring to Timoshenko and Gere.[12]

Accuracy, which is inferred in the above restrictions, is also dependent upon the manner of load application, beam geometry, loading fixtures, and surface preparation. Although specimen size will not affect accuracy except for extremely small geometries, it will alter the magnitude of the stress level at failure, and this must also be considered. These subjects are discussed in the following paragraphs, and guidelines for specimen geometry and minimization of errors are provided.

First to be considered, however, are the merits of a four-point beam loading system as compared to the three-point beam loading system.

11. RITTER, J. E., and WILSON, W. R. D. *Friction Effects in Four-Point Bending.* ASLE Transactions, v. 18, no. 2, p. 130-134, presented at the 29th Annual Meeting, April 28-May 2, 1974.
12. TIMOSHENKO, S., and GERE, J. M. *Theory of Elastic Stability.* McGraw-Hill Book Co., Inc., New York, 1961.

FOUR-POINT AND THREE-POINT LOADING

The bending moment, from which the desired fracture stress is computed in an idealized four-point beam loading system, as shown in Figure 1a, is constant, and there are no horizontal or vertical shear stresses within the inner span. However, the bending moment in an idealized three-point beam loading system, shown in Figure 2a, is linearly dependent upon the distance from the nearest support to the fracture origin, and thus requires an additional distance measurement to determine the fracture stress. Also, the shear stresses for the three-point beam loading system are developed over the full span, thus deviating from the ideally sought uniaxial stress state present in the four-point beam loading system.

Wedging stresses[4] occur under all points of load application during flexure testing of beams. The effect of the wedging stress occurring at the inner load points of a four-point beam test is to cause a deviation from the idealized calculated constant stress at the two local regions. However, if the ratio of half the distance between the outer span L and inner span ℓ, called a, to beam depth d is great enough,* the stress reduction will not only be small but will decay rapidly, and the stress predicted by simple beam theory will be developed. Yet, the maximum stress computed by simple beam formula for the three-point beam system is never attained. The actual maximum stress occurs at a short distance either side of the center of the load application point, which can cause fracture at these sites, rather than at the center, according to Rudnick et al.[13] This observation has also been confirmed by Oh and Finnie,[14] where only for a material with no scatter in strength will the fracture location of a three-point loaded beam be theoretically† located at the center load point.

Brittle materials are affected by size. Compensation can be realized through the use of statistical analysis offered by Weibull.[15] Although the four-point beam system assures a simple stress state which is easier to analyze[15] than the more complex biaxial stress state associated with the three-point beam specimen, this will be less of a consideration if the beam is designed properly. Nevertheless, the three-point loaded beam system is preferred when investigating material or process development, because of smaller specimen size, or when attempting to pinpoint fracture origin location.‡ On the other hand, the four-point loaded beam is preferred when determination of strength for design purposes is desired, because the center span is uniaxially stressed, i.e., no shear stresses exist. It is concluded that each of these systems is suited for a particular application and each has different advantages and disadvantages.

Each of these beam systems will be subjected to external influences which will affect the accuracy of the test results. These external influences, directly or indirectly caused by the application of loads through the test fixtures, will lead to either configuration constraints or errors.

*This requirement will be discussed subsequently.

†In Reference 14, the authors considered only a statistical analysis and ignored wedging stress considerations.

‡Private communication with R. W. Rice of N. R. L.

13. RUDNICK, H., MARSCHALL, C. W., DUCKWORTH, W. H., and ENRICK, B. R. *The Evaluation and Interpretation of Mechanical Properties of Brittle Materials.* AFME TR 67-316, April 1968.

14. OH, H. L., and FINNIE, I. *On the Location of Fracture in Brittle Solids - I, Due to Static Loading.* Int. J. of Fracture Mechanics, v. 6, no. 3, September 1970, p. 287-300.

15. WEIBULL, W. *Statistical Theory of Strength of Materials.* Royal Swedish Institute for Engineering Res., Proc. no. 151, 1939, p. 1-45.

ERRORS FROM EXTERNAL INFLUENCES

The major influence on the accurate determination of flexure strength of a beam in bending arises from the application of load through the fixtures to the specimen. The idealizations indicated in Figures 1a and 2a are rarely met, and usually tests are conducted using a convenient rigid loading head and support member as depicted in Figures 1b and 2b. The constraints on either the loading fixture or the specimen and/or errors resulting from such fixture designs are many. Such constraints or errors, which are discussed in turn, are caused by:

1. eccentric loading
2. span dimensions
3. beam twisting
4. friction
5. contact stresses
6. wedging stresses
7. beam overhang
8. contact point tangency shift
9. specimen preparation
10. load readout
11. specimen dimension measurement

Eccentric Loading

a. Four-Point Loaded Beams

When calculating bending stress by simple beam theory formula for four-point loaded beams, it is usual to assume that the moment within the inner span ℓ is constant. However, if a loading head that can only translate is used, as idealized in Figure 1b, it is impossible to attain this idealized moment condition when $x_1 \neq x_3 - x_2$;[13,16] this is shown in Figure 1c. The ratio of σ_x/σ_b, from Appendix B, is:

$$\sigma_x/\sigma_b = \left[\frac{P_1}{(P_2 + P_3)/?} \right] x_1/a \quad . \tag{9}$$

The loads and distances are also shown in Figure 1c, and a is the value of a_1 with perfect load location. The error is magnified by the ratio of x_1/a. (Of course, if $P_1 = P_2 = P_3$, which implies exact location of the points of load application, there is no error.) In order to estimate the magnitude of such an error it was assumed in

16. HOAGLAND, R. G., MARSCHALL, C. W., and DUCKWORTH, W. H. *Reduction of Errors in Ceramic Bend Tests.* J. Amer. Cer. Soc., v. 59, no. 5-6, May-June 1976, p. 189-192.

Appendix B that the upper two load points in Figure 1c were at a fixed distance $x_2 - x_1 = \ell$ and were constrained to translate vertically during loading, and that the loading head would be located such that $x_1 \neq x_3 - x_2$. This method of loading, being the most convenient, is often adopted by many investigators, and therefore the resulting error determination is not unrealistic.

The analysis was accomplished by simply enforcing the condition that the displacement at x_1 must be equal to the displacement at x_2 in the deflection equation. This results in the following relationships between σ_x and σ_b in terms of the load eccentricity ratio e/L (see Appendix B for details):

$$\sigma_x/\sigma_b = \frac{[(e/L + a/L)/(a/L)][1-(e/L + a/L) - \ell/L]\{(\ell/L)[2-(e/L + a/L)]-2[1-(e/L + a/L)]^2\}}{3(e/L + a/L)[1- \ell/L -(e/L+ a/L)]-(1- \ell/L)^2} \tag{10}$$

where the parameter a defined as $(L-\ell)/2$, e defined as (a_1-a); and ℓ and L are shown in Figure 1.

Most workers in the testing field utilize either a 1/3-point ($a/L = 1/3$ and $\ell/L = 1/3$) or a 1/4-point ($a/L = 1/4$ and $\ell/L = 1/2$) loading. Thus by substitution of these parameters into Equation 10, we obtain:

$$(\sigma_x/\sigma_b)_{\ell/L=\frac{1}{3}} = \frac{[3(e/L)+1](1/3 - e/L)[1/3(5/3 - e/L)-2(2/3 - e/L)^2]}{[3(e/L)+1](1/3 - e/L) - 4/9} \tag{11}$$

$$(\sigma_x/\sigma_b)_{\ell/L=\frac{1}{2}} = \frac{[4(e/L)+1](1/4 - e/L)[1/2(7/4 - e/L)-2(3/4 - e/L)^2]}{[3(e/L) + 3/4](1/4 - e/L) - 1/4} \tag{12}$$

The reader is cautioned that for given values of ℓ/L there exists a limit on e/L in (10), (11), and (12); that is, if a_1 is such that either P_2 or $P_3 = 0$, the test system changes from four-point to an eccentric three-point loading (see Appendix B), and the above equations become invalid.

The error, defined as $[(\sigma_b - \sigma_x)/\sigma_x]100$, was determined from (11) and (12) for the 1/3-point and 1/4-point loaded beams and is shown in Tables 5 and 6 as a function of e/L. Only negative values of e/L were considered in (11) and (12) because when $e/L < 0$, $\sigma_x > \sigma_b$. A negative value of e/L corresponds to the inner load bearing which is offset closer to the outer load bearing ($a_1 < a$). An error of similar magnitude, but larger and of opposite sign, exists at the other inner load bearing, which is why Tables 5 and 6 show $\pm$ values. Tables 5 and 6 show that for corresponding e/L, when $a_1/L \neq a_2/L$, the 1/3-point loading system results in lesser error than the 1/4-point loading system. Also, in accordance with the above discussion, e/L in Tables 5 and 6 is limited to a range of ± 0.0443 and ± 0.0465. The errors indicated in these tables can be minimized by designing the loading fixture so that the inner and outer spans are independently fixed. Also, the inner span should be designed with accurate location adjustment and allowed to pivot as recommended by Hoagland et al.[16]

Table 5. ERROR DUE TO ECCENTRIC LOAD APPLICATION FOR A 1/3-FOUR-POINT LOADED BEAM, FOR EITHER A NON-PIVOTING OR PIVOTING LOADING HEAD

When $\ell/L = 1/3$ and $a_1/L \neq a_2/L$

$e/L = \pm(a_1/L - 1/3)$	NON-PIVOTING ± % Error	PIVOTING ± % Error
0.0	0.0	0.0
0.0010	0.7	0.1
0.0019	1.3	0.2
0.0038	2.6	0.4
0.0057	3.8	0.6
0.0076	4.9	0.7
0.0095	6.0	0.9
0.0114	7.0	1.1
0.0133	8.1	1.2
0.0333	16.1	2.6
0.0433	18.7	3.1
0.0443	18.9	3.2

Table 6. ERROR DUE TO ECCENTRIC LOAD APPLICATION FOR A 1/4-FOUR-POINT LOADED BEAM, FOR EITHER A NON-PIVOTING OR A PIVOTING LOADING HEAD

When $\ell/L = 1/2$ and $a_1/L \neq a_2/L$

$e/L = \pm(a_1/L - 1/4)$	NON-PIVOTING ± % Error	PIVOTING ± % Error
0.0	0.0	0.0
0.0010	1.0	0.2
0.0020	2.1	0.4
0.0040	3.8	0.8
0.0080	7.1	1.5
0.0120	10.0	2.2
0.0160	12.6	2.9
0.0200	14.7	3.6
0.0240	16.6	4.2
0.0280	18.3	4.7
0.0320	19.8	5.3
0.0340	20.8	5.6
0.0400	21.8	6.3
0.0465	22.9	7.0

Many flexure fixtures do permit the loading head to translate and pivot. The eccentric loading error in this instance will be due to the actual moment being different from the assumed moment. If the beam deflection is small, the angular rotation of the loading head can be ignored and the maximum bending stress can be determined utilizing force and moment equilibrium:

$$\frac{\sigma_x}{\sigma_b} = 1 - \frac{2e}{L} + \frac{e}{a} - \frac{2e^2}{aL} \tag{13}$$

The maximum stress will exist under the inner load bearing which is offset to give a larger moment arm (a). A similar error (for $e/L \leq 0.01$), but larger and of opposite sign, will exist at the opposite inner load bearing. Substituting for either 1/3 or 1/4-point loading:

$$\left(\frac{\sigma_x}{\sigma_b}\right)_{\ell/L=1/3} = 1 + \frac{e}{L} - \frac{6e^2}{L^2} \tag{14a}$$

$$\left(\frac{\sigma_x}{\sigma_b}\right)_{\ell/L=1/4} = 1 + \frac{2e}{L} - \frac{8e^2}{L^2} \tag{14b}$$

The latter expression was also derived by Jayatilaka.[17] These errors at the point of maximum stress are also given in Tables 5 and 6 for comparison. It is evident that a translating and pivoting loading head is preferred to a rigid loading head because the errors are appreciably less. This finding is consistent with recommendations of Hoagland et al.[16]

17. JAYATILAKA, A. DeS. *Fracture of Engineering Brittle Materials.* Applied Science Publishers, LTD, London, 1979, p. 187.

b. Three-Point Loaded Beams

The ratio of σ_x to σ_b is:

$$\frac{\sigma_x}{\sigma_b} = 1 - 4\left(\frac{e}{L}\right)^2 \tag{15}$$

The percent error as a function of e/L is given in Table 7. Notice that the percent errors in Table 7 are always positive, and when the load application point is misplaced, such errors are much less than those of equivalent e/L values shown in Tables 5 and 6 for the four-point loaded beams. Notice also that when $\pm e/L = 0.500$, the error is infinite, i.e., the three-point loading model is no longer valid.

Table 7. ERROR DUE TO ECCENTRIC LOAD APPLICATION FOR A THREE-POINT LOADED BEAM

When $a_1/L \neq a_2/L \neq 1/2$
$e/L = 1/2 - a_1/L$

±e/L	% Error
0	0
0.025	0.25
0.050	1.0
0.075	2.3
0.100	4.2
0.150	9.9
0.200	19.0
0.250	33.3
0.300	56.3
0.400	177.8
0.450	426.3
0.500	∞

Note: All errors are positive.

Span Dimensions

a. Four-Point Loaded Beams

An additional mislocation error may exist if the inner bearing span (ℓ) or the outer bearing span (L) are not their prescribed values, even if they are properly centered with respect to each other. This will alter the moment arm (a). Assuming the inner span is actually $\ell + e_s$ and the outer span is $L - e_s$, then the ratio of σ_x to σ_b is:

$$\frac{\sigma_x}{\sigma_b} = 1 - [2e_s/(L - \ell)] \tag{16}$$

where e_s is the error of the inner and outer span dimensions. A similar error (for $e_s/L \leq 0.01$), but of opposite sign exists if the inner span is $\ell - e_s$ and the outer span is $L + e_s$. Errors are tabulated in Table 8 for the 1/3 and 1/4-point loaded beams. The largest error magnitude, occurring when the outer span is $L - e_s$, is reported in these tables.

Table 8. ERROR DUE TO WRONG SPANS

	± % Error		
$\pm e_s/L$	1/3-Four-Point	1/4-Four-Point	Three-Point
0	0	0	0
0.001	0.3	0.4	0.1
0.002	0.6	0.8	0.2
0.005	1.5	2.0	0.5
0.010	3.1	4.2	1.0
0.015	4.7	6.4	1.5
0.020	6.4	8.7	2.0
0.025	8.1	11.1	2.6
0.050	17.6	25.0	5.3

Note: All errors are either positive or negative.

b. Three-Point Loaded Beams

A simple analysis shows that if the support span is actually $L - e_s$, then:

$$\frac{\sigma_x}{\sigma_b} = \frac{L - e_s}{L} \tag{17}$$

The error in determining the stress is given in Table 8. If the support span is $L+e_s$, a similar error occurs but it is slightly less and of opposite sign. A comparison of Equations 16 and 17 shows that the four-point configuration amplifies the span error, whereas the error in computing the stress for a three-point beam is nearly the same as the span error.

Beam Twisting

A net torque can result from line loads being nonuniform or nonparallel between pairs of load contact points or if the cross section of the specimen is skewed over its length.[13,16]

Such a skewed condition is shown schematically in Figure 3 for a four-point bending specimen. The error due to twisting has been estimated for plane strain and plane stress conditions by examining the maximum principal stress due to bending and torsion and comparing it to the bending stress.[16] "Bottoming" of the specimen on the fixture was not considered. Bottoming occurs when the bearing rollers contact the specimen across its full width. For the sake of completeness, bottoming is considered in the analysis given in Appendix C. The maximum principal stress, assuming a plane strain condition, is derived in Reference 1. The plane strain criterion leads to slightly higher error estimates, but the plane stress criterion is more appropriate. The plain stress solution is also given in Reference 16, but the analysis has been extended in this report to incorporate the case where the specimen bottoms on the fixture.

The maximum principal stress for either a skewed four-point or three-point beam in bending, considering a plane stress condition, is given by:

$$\sigma_{n_{max}} = \sigma_b/2\{1 + (1/3k_2)[(nb/\ell')^2 + 9k_2^2]\}^{1/2} \tag{18a}$$

where σ_b is the apparent bend strength and ℓ' is either equal to "a" for four-point bending or equal to L/2 for three-point bending. Also:

$$n = [3k_1(e/\sigma_b)/(1 + \nu)][(d/L_T)\phi_s + (d/\ell')\phi_F]\left(\frac{\ell'}{b}\right) \qquad (18b)$$

where for Case I: n = 1, failure occurs prior to bottoming of the specimen in the loading fixture, and for Case II: n < 1, failure occurs after bottoming.

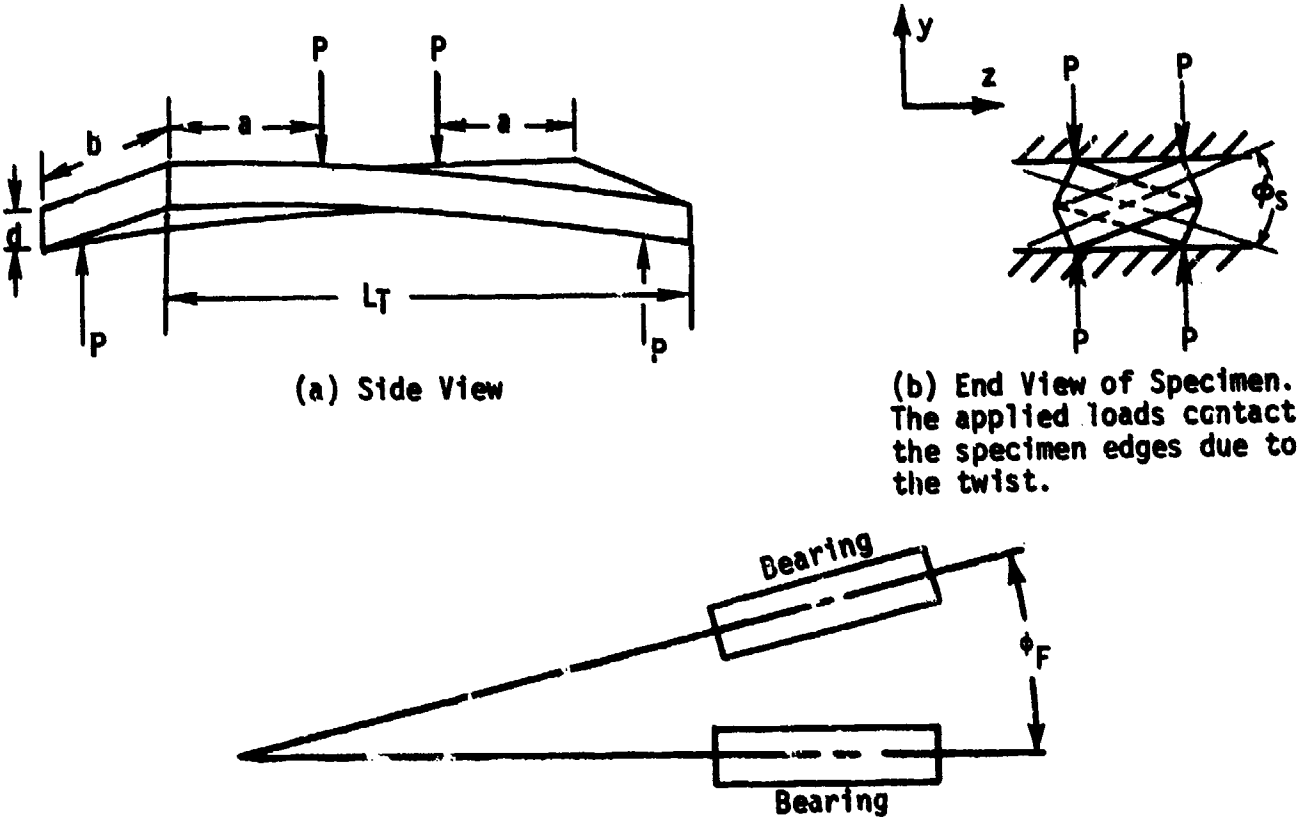

(a) Side View

(b) End View of Specimen. The applied loads contact the specimen edges due to the twist.

(c) End View of Fixture Showing ϕ_F, the Fixture Twist Angle Between a Pair of Contact and Load Bearings

Figure 3. Twisting of a four-point beam specimen.

The factors k_1 and k_2, obtained from Reference 3 and given in Table 9, are numerical values associated with the torsional stress component which are dependent on the ratio of b/d. The measured angle of twist (or skew angle) along the total length L_T of the specimen is ϕ_s (see Figure 3c), and along the fixture from one support point to the adjacent load point is ϕ_F.

The maximum principal stress as given by (18a) can be utilized to determine the percent error for various ratios of n, ℓ'/b, and b/d. This was accomplished and is shown in Table 10. Notice that the range of n varies from 0.20 to 1.00. It is expected that if bottoming does not occur prior to fracture because of an excessive twist angle, the maximum ratio of n that can be attained is 1.0 and thus the tables do not accommodate n > 1.0.

Table 9. k_1 AND k_2

b/d	k_1	k_2
1.0	0.1406	0.208
1.2	0.166	0.219
1.5	0.196	0.231
2.0	0.229	0.246
2.5	0.249	0.256
5.0	0.291	0.291
10.0	0.312	0.312
∞	0.333	0.333

Table 10. ERROR DUE TO BEAM TWISTING PLANE STRESS ASSUMPTION*

$\nu = 0.25$

		b/d					
	ℓ'/b	1.0	1.2	1.5	2.0	2.5	5.0
n = 0.20	1.0	2.44	2.22	2.00	1.77	1.62	1.27
	2.0	0.63	0.57	0.52	0.46	0.42	0.32
	2.5	0.41	0.37	0.33	0.29	0.27	0.21
	5.0	0.10	0.09	0.08	0.07	0.07	0.05
	10.0	0.03	0.02	0.02	0.02	0.02	0.01
	∞	0	0	0	0	0	0
n = 0.40	1.0	8.57	7.87	7.18	6.44	5.93	4.75
	2.0	2.44	2.22	2.00	1.77	1.62	1.27
	2.5	1.59	1.44	1.30	1.15	1.05	0.82
	5.0	0.41	0.37	0.33	0.29	0.27	0.21
	10.0	0.10	0.09	0.08	0.07	0.07	0.05
	∞	0	0	0	0	0	0
n = 0.60	1.0	16.20	15.05	13.09	12.63	11.74	9.61
	2.0	5.19	4.73	4.29	3.82	3.51	2.78
	2.5	3.44	3.13	2.83	2.52	2.30	1.82
	5.0	0.91	0.82	0.74	0.65	0.60	0.47
	10.0	0.23	0.21	0.19	0.16	0.15	0.12
	∞	0	0	0	0	0	0
n = 0.80	1.0	23.81	22.36	20.87	19.20	18.01	15.09
	2.0	8.57	7.87	7.18	6.44	5.93	4.75
	2.5	5.82	5.32	4.83	4.31	3.95	3.14
	5.0	1.59	1.44	1.30	1.15	1.05	0.82
	10.0	0.41	0.37	0.33	0.29	0.27	0.21
	∞	0	0	0	0	0	0
n = 1.0	1.0	30.74	29.12	27.43	25.50	24.11	20.61
	2.0	12.32	11.38	10.44	9.42	8.72	7.06
	2.5	8.57	7.87	7.18	6.44	5.93	4.75
	5.0	2.44	2.22	2.00	1.77	1.62	1.27
	10.0	0.63	0.57	0.52	0.46	0.42	0.32
	∞	0	0	0	0	0	0

Note: All errors are negative.
*An error table based upon plain strain conditions is in Reference 1.

Friction

It has already been shown in Table 4, for the two beam systems considered, that the error due to deflection will be negligible if $L/d \leq 25$. It appears that this limit is well within an attainable realistic geometry ratio. Therefore, the friction effect at the load and support points will be minimized with respect to large deflections. This also implies that there will be no effect from friction on the contact tangency shift. (These factors will be discussed subsequently.) However, friction will cause a moment acting out of the plane of the beam that can not be ignored. This factor is considered in the following.

When determining bend strength by simple beam theory, it is usual to assume that the supports and load points are frictionless, whereas in fact they are not. The presence of friction in flexure tests with fixed load and support points gives rise to couples at such locations as well as axial forces at the neutral axis of the beam. The net axial force is relatively small and therefore is ignored here. However, if the moment is not corrected to account for the couple in the determination of flexure stress, an error will result. Error equations adapted from the results* available in the literature[16-19] are given below for the four-point and three-point loading systems:

$$\bar{\epsilon} = 100\left(\frac{\mu}{a/d - \mu}\right) \tag{19}$$

and

$$\bar{\epsilon} = 100\left(\frac{\mu}{L/2d - \mu}\right) \tag{20}$$

Such errors as defined by the above equations can be significant, according to References 16, 19 and 20. Newnham[19] and Weil[20] reported that the experimental difference in failure stress using rigid knife edges as compared to roller-type contact points was as high as 12% for silicon nitride and 13% for graphite.

Contact Stresses

Loads on bend specimens applied through knife edges or small-diameter rollers result in high stresses under these line loads. High compressive contact stresses can result and cause local crushing. (Also, shear stress near the locality of the load point can be several times higher than that predicted by beam theory.)

Reference 4 gives equations for determining the contact pressure between a cylinder (or roller) and a flat surface (see Figure 4) as a function of the applied load, modulus of each material, and the roller radius. If it can be assumed that the two materials are identical and that the allowable bearing pressure or contact pressure can be as high as twice the bend strength of the material, then limits on the roller radius for both loading systems will result. For example, from Reference 4 we have:

*Beam width constraint occurs also because of friction transverse to the beam's long axis. However, this effect (see Newnham[19]) is small and thus not considered here.

18. DUCKWORTH, W. H., et al. *Mechanical-Property Tests on Ceramic Bodies.* WADC TR 52-67, March 1952, p. 67-70.
19. NEWNHAM, R. C. *Strength Tests for Brittle Materials.* Proc. of the British Cer. Soc., no. 25, May 1975, p. 281-293.
20. WEIL, N. A. *Studies of Brittle Behaviour of Ceramic Materials.* ASD TR 61-628, Part II, April 1962, p. 38-42.

$$p_{max} = 0.59\sqrt{PE/2b\rho_1} \qquad (21)$$

where p_{max} is the maximum contact pressure. (Note that the roller radius can be either ρ_1 or ρ_2.) However, we shall assume that $p_{max} \leq 2\sigma_b$. Also for four-point loading, $\sigma_b = 6Pa/bd^2$, and for three-point loading, $\sigma_b = (3/2)PL/bd^2$. Substituting of σ_b into (17) and solving for ρ_1/d we obtain

$$\rho_1/d \geq 7.25\ d/a \text{ for the four-point loaded beam, and} \qquad (22a)$$

$$\rho_1/d \geq 29.0\ d/L \text{ for the three-point loaded beam,} \qquad (22b)$$

where it was assumed that $E/\sigma_b = 1000$. Of course, if the specimen and bearing are made of different materials, and if E/σ_b is not 1000, then further calculations are required to ensure that the ceramic doesn't locally crush or fracture, or that the bearing does not permanently flatten.

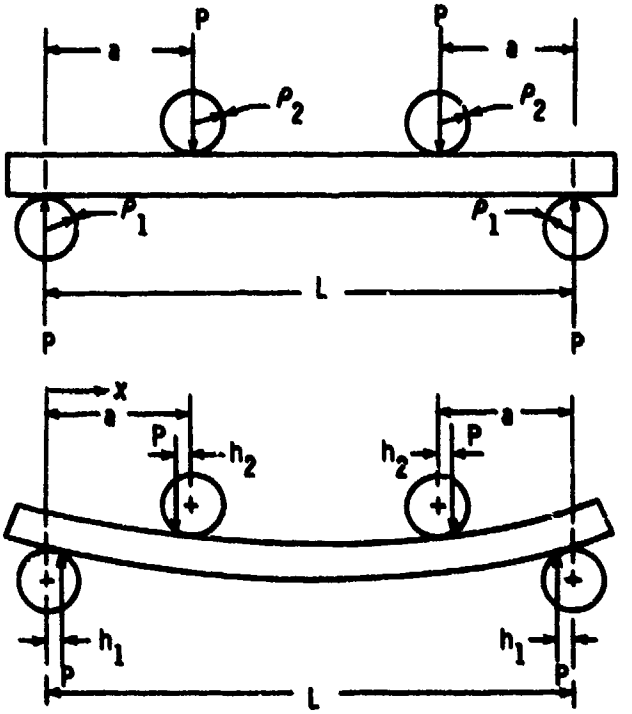

Figure 4. Contact point tangency shift.

Wedging Stresses

Localized contact at the load bearings can cause a more subtle problem, which is referred to as wedging stresses. The effect of the wedging stress is to provide a substantial tensile stress contribution at the compressive side of the beam adjacent to the load points. A net tensile stress can not be created if $d/2\ell' < 1$, according to Reference 16. More importantly, a tensile stress is added to that already present due to beam bending at the tensile side of the beam, thereby causing a deviation from the assumed stress calculated by simple beam theory.

This problem is generally treated in Reference 3 and particular results from von Kármán and Seewald[21] for a similar situation are used to estimate this error. An analysis for this error is given in Appendix D. The resulting error determinations for four- and three-point loaded beams are given in Table 11. In the calculation of the errors, which are a function of a/d or L/d, as well as x'/d, the computed σ_b corresponds to the failure site location (x'/d).

Table 11. ERROR DUE TO WEDGING

Loading	x'/d* 0	0.125	0.25	0.375	0.50	0.75	1.0	1.50
a. Four-point, a/d								
1.0	+4.7	-0.5	-2.8	-2.1	-1.4	-0.7	-0.3	†
1.5	+3.1	-0.3	-1.9	-1.4	-0.9	-0.5	-0.2	0
2.0	+2.3	-0.2	-1.4	-1.1	-0.7	-0.4	-0.2	0
3.0	+1.5	-0.2	-1.0	-0.7	-0.5	-0.2	-0.1	0
4.0	+1.1	-0.1	-0.7	-0.5	-0.3	-0.2	-0.1	0
5.0	+0.9	-0.1	-0.6	-0.4	-0.3	-0.1	0	0
6.0	+0.8	-0.1	-0.5	-0.4	-0.2	-0.1	0	0
8.0	+0.6	0	-0.4	-0.3	-0.2	-0.1	0	0
10.0	+0.4	0	-0.3	-0.2	-0.1	-0.1	0	0
15.0	+0.3	0	-0.2	-0.1	-0.1	0	0	0
20.0	+0.2	0	-0.1	-0.1	-0.1	0	0	0
40.0	+0.1	0	-0.1	-0.1	0	0	0	0
60.0	+0.1	0	0	0	0	0	0	0
∞	0	0	0	0	0	0	0	0
b. Three-point, L/d								
1.0	+21.6	-2.4	-18.8	-25.4	†	†	†	†
1.5	+13.4	-1.4	-10.4	-10.2	-10.1	†	†	†
2.0	+9.7	-1.0	-7.2	-6.4	-5.3	-5.5	†	†
3.0	+6.3	-0.7	-4.4	-3.7	-2.7	-1.9	-1.3	†
4.0	+4.7	-0.5	-3.2	-2.6	-1.8	-1.2	-0.6	-0.1
5.0	+3.7	-0.4	-2.5	-2.0	-1.4	-0.8	-0.4	0
6.0	+3.1	-0.3	-2.1	-1.6	-1.1	-0.6	-0.3	0
8.0	+2.3	-0.2	-1.5	-1.2	-0.8	-0.4	-0.2	0
10.0	+1.8	-0.2	-1.2	-0.9	-0.6	-0.3	-0.2	0
15.0	+1.2	-0.1	-0.8	-0.6	-0.4	-0.2	-0.1	0
20.0	+0.9	-0.1	-0.6	-0.4	-0.3	-0.2	-0.1	0
40.0	+0.4	0	-0.3	-0.2	-0.1	-0.1	0	0
60.0	+0.3	0	-0.2	-0.1	-0.1	-0.1	0	0
∞	0	0	0	0	0	0	0	0

*x' is the distance on either side of the load contact point where failure occurs.

†Location is at or beyond outer span limit.

Beam Overhang

The overhangs of the beam must be great enough so that the local stresses at the beam support points are not amplified due to beam-end effects. These stresses are dampened out within a distance equal to one beam depth.[21] Thus, by allowing

$$L_T \geq L + 2d \tag{23}$$

beam-end effects are avoided.

21. VON KÁRMÁN, T., and SEEWALD, F. Alhandl Aerodynam, Inst. Tech. Hochschule, 1946, p. 256.

Contact Point Tangency Shift

Significant changes in span length can occur in both four-point and three-point loading systems if contact radii of support and load points are large compared to beam depth. The shift in point of tangency, as shown by h_1 and h_2 in Figure 4, is a function of the contact radii, specimen thickness, and the ratio of the modulus of elasticity to the bend strength. For materials that behave elastically, such as those considered here, the change in tangency point and thus the error arising because of the change in moment arm from the ideal can be predicted mathematically for linear systems. This is accomplished and is presented in Appendix E. The approach was patterned after Westwater[22] who corrected for span shortening but ignored friction at the support points of a three-point loaded beam.*

In Appendix E the formulas are derived for a four-point loaded beam and then reduced to the special case of a three-point loaded beam. These results are put in terms of error functions assuming the simple beam theory is applied without correcting for span shortening, as in the case of the lower support, and span lengthening between the upper loading points shown in Figure 4.

The errors are determined for four-point loaded beams of 1/3 and 1/4 loading points as a function of ρ_1/d and ρ_2/d, and the three-point loaded beam as a function of ρ_1/d only. These errors are given in Table 12, where it was assumed that $E/\sigma = 1000$.

Table 12. % ERROR DUE TO TANGENCY POINT SHIFT

$E/\sigma_b = 1 \times 10^3$

Loading	ρ_1/d	ρ_2/d 1.0	2.0	5.0	10.0
a. Four-point, a/L = 1/3	1.0	0.3	0.4	0.7	1.2
	2.0	0.5	0.6	0.9	1.4
	4.1	0.9	1.0	1.3	1.8
	6.1	1.3	1.4	1.7	2.3
	8.2	1.7	1.8	2.1	2.7
	10.3	2.1	2.2	2.6	3.1
b. Four-point, a/L = 1/4	0.67	0.4	0.6	1.2	2.2
	1.35	0.6	0.8	1.4	2.5
	2.7	1.0	1.2	1.8	2.9
	4.1	1.4	1.6	2.2	3.3
	5.5	1.8	2.0	2.6	3.7
	6.9	2.2	2.4	3.1	4.1
c. Three-point, a/L = 1/2	1.0	0.1	Regardless of ρ_2/d value		
	2.0	0.2			
	4.0	0.4			
	6.0	0.6			
	8.0	0.8			
	10.0	1.0			

Note: All errors are positive.

*Westwater also determined an approximate relationship for the horizontal load arising because of tangency shift. However, for beams of small deflection, the error is negligible.

22. WESTWATER, J. W. *Flexure Testing of Plastic Materials.* Proc. ASTM, v. 49, 1949.

Specimen Preparation

The flexure strength of each brittle material is not only supersensitive to the final surface finish because the maximum tensile stress occurs at the beam surface, but is also highly sensitive to prior finish history. For this reason it is impossible to specify an optimum surface finish procedure for all brittle materials, so that failure will be due to inherent flaws related to the material or material processing, rather than an imposed defect resulting from the finish process. Indeed, the designer or materials developer may not be able to specify a particular finish procedure. Therefore, rather than attempt to dictate surface finish requirements, it is suggested that each set of reported test data results be accompanied by surface finish history and/or material process history, whichever is applicable.

There are, however, several specific recommendations related to surface finishing procedures that can be presented. Corner flaws resulting from chipping or cracking during the grinding operation are sources of low-strength failure. Rounding or beveling of the corner as depicted in Figure 5 appears to reduce premature failure.[23] Since a chamfer will double the number of edges, thus doubling the source of flaw locations, rounding is preferred.[24] Also, it is important to grind the edges and flat surfaces[24] by a motion parallel to, rather than perpendicular to, the specimen length. It is further indicated[23] that finishing of the corner should be comparable in all aspects to that applied to the beam surfaces.

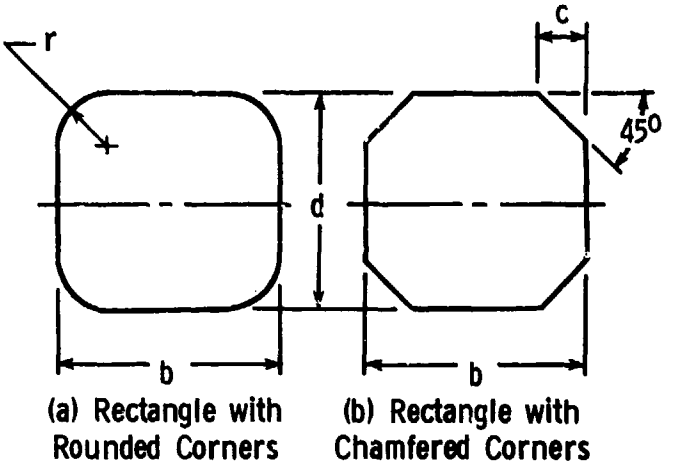

Figure 5. Beam cross section.

If the corner radii or chamfer is small, the error in ignoring the change in moment of inertia will be negligible. The limiting ratio of corner radii or 45° chamfer dimension to beam depth can be determined from the error analysis due to neglecting the change in moment of inertia given in Appendix F. This error in determining flexure stress, when neglecting corner radii or 45° chamfer, is given in Table 13.

23. RICE, R. W. *Machining of Ceramics.* Proc. of the Second Army Materials Technology Conference - Ceramics for High Performance Applications, J. J. Burke, A. E. Gorum, and R. N. Katz, ed., Brook Hill Publishing Company, Chestnut Hill, Massachusetts, 1974.
24. RICE, R. W. *The Effect of Grinding Direction on the Strength of Ceramics.* The Science of Ceramics Machining and Surface Finishing, S. J. Scheider and R. W. Rice, ed., NBS Special Publication 348, Washington, DC, Government Printing Office (SD Catalog No. 13.10:348), 1972, p. 365-376.

Table 13. % ERROR IN DETERMINING FLEXURE STRESS

a. When neglecting corner radii

r/d	b/d = 1.0	2.0	4.0
0	0	0	0
0.02	0.1	0.1	0
0.04	0.4	0.2	0.1
0.06	0.9	0.4	0.2
0.08	1.5	0.8	0.4
0.10	2.4	1.2	0.6
0.15	5.1	2.5	1.3
0.20	8.6	4.3	2.2

b. When neglecting 45° chamfer

c/d	1.0	2.0	4.0
0	0	0	0
0.01	0.1	0.1	0.1
0.02	0.2	0.1	0.1
0.03	0.5	0.3	0.1
0.04	0.9	0.5	0.2
0.05	1.4	0.7	0.4
0.06	2.0	1.0	0.5
0.08	3.4	1.7	0.9
0.10	5.2	2.6	1.3

Note: All errors are negative.

Load Readout

It is readily apparent that an error in the break load P is identically carried over as an error in the stress σ_b.

Specimen Dimension Measurement

It is further evident that an error in measuring the specimen dimension can also lead to an error in stress. It is recommended that the cross section dimensions b and d be measured at the point of failure (to preclude specimen taper effects). Considering the true specimen dimension to be in error by e_m, then from Equations 1a or 1b:

$$\frac{\sigma_x}{\sigma_b} = \frac{bd^2}{(b + e_m)(d + e_m)^2} \quad \text{for three- or four-point flexure.} \tag{24}$$

If e_m is small relative to b or d:

$$\bar{\varepsilon} = \pm\left[2\left(\frac{e_m}{d}\right) + \left(\frac{e_m}{b}\right)\right] \tag{25}$$

Equation 25 shows that, if the measurement error is expressed as e_m/b or e_m/d, the error in stress is magnified. For example, if d = b, then a 1% error in specimen measurement becomes a 3% error in stress.

RECOMMENDATIONS FOR FLEXURE TESTING

It is beyond the scope of this report to analytically determine the intersection of errors to arrive at a total stress error. Nevertheless, a range of practical geometry ratios and error tolerances can be specified so that a simple additive stress error is a few percent at most. The recommendations are summarized in Table 14 and are discussed below.

Several of the error sources are negligible for most common test configurations. These include initial beam curvature, anticlastic curvature, beam overhand and large deflection sources. The error due to nonhomogeneity are largely unknown at this time.

Many of the errors are independent of the test configuration but should not be overlooked. Micrometers are readily available that are accurate to within 0.0025 mm (0.0001"), and these should be used to keep specimen dimension measurement errors to a few tenths of a percent. Many conventional universal testing machines can easily read break load to within 0.5%. Corner chamfers should not be casually applied to specimens, particularly ones with small cross sections, since the error can be significant. The analysis in this report assumes the chamfers were identical. If they are not, or if only two chamfers are used, a further error can result due to a shift in the position of the specimen's neutral axis.

Some of the more important error sources do depend upon the fixture configuration. The 1/3-four-point mode has somewhat less error than the 1/4-four-point mode for the cases of wrong span and contact tangency shift sources. A greater difference exists for the eccentric loading source of error. Special care should be taken to minimize wrong spans or eccentric loading error sources in four-point flexure since an error in such fixture positioning is magnified as an error of stress. Three-point loading is much less sensitive to load bearing position error sources than four-point loading. On the other hand, a three-point loaded beam is adversely affected by the presence of wedging stresses at the point of maximum stress. These wedging stresses decay rapidly with distance away from the load bearings and will have considerably less influence on four-point testing. The bearing friction error can be of large magnitude for either three- or four-point loading, and it is strongly recommended that the load bearings be mounted such that they are free to rotate. Twisting error, due to lack of parallelism of fixture bearings or specimen surfaces, is harder to predict, because the error is dependent upon many geometry terms as well as the specimen stiffness. Parallelism requirements are more important for four-point loading than three-point. For most geometries and materials, parallelism limits of better than 1^{o} in the specimen and also the fixtures are needed to keep the error within 1 percent.

There are two conflicting requirements regarding contact radius at the loading and support points: the first is that radii must be great enough so that contact or bearing pressure does not cause local failure of the beam; the second is that the contact radii be small enough so that the error due to contact point tangency shift is not great.

Many of the error analyses in this report assumed the ratio of elastic modulus to bend strength (E/σ) was 1000. Values could, in fact, range from 100 to 2500. In general, the larger E/σ, the larger will be the twisting error and load bearing contact stress, but the lesser will be the contact tangency shift and large deflection errors.

Table 14. ERROR SOURCES AND RECOMMENDATIONS

Error Source		Recommendations	Error ε (%)
$E_t \neq E_c$; Nonhomogeneity & Anisotropy (Table 1)		Error depends upon material and on a fabrication process.	---
Initial Beam Curvature (Table 2)		$\rho_c/d \geq 100$	$\leq$-0.3%
Anticlastic Curvature (Table 3)		$b/d \leq 75$	0
Large Deflection (Table 4)	Four-Point	$a/d \leq 12.5$	$\leq$-0.1
	Three-Point	$L/d \leq 25$	$\leq$-0.1
Eccentric Load (Tables 5-7)	1/3 Four-Point	Non-Pivoting Head $e/L < 0.001$	$<\pm$0.7
		Pivoting Head $e/L < 0.002$	$\pm$0.2
	1/4 Four-Point	Non-Pivoting Head $e/L < 0.001$	$<\pm$1.0
		Pivoting Head $e/L < 0.002$	$<\pm$0.4
	Three-Point	$e/L < 0.025$	$<+0.25$
Wrong Span (Table 8)	1/3 Four-Point	$e_s/L < 0.001$	$<\pm$0.3
	1/4 Four-Point	$e_s/L < 0.001$	$<\pm$0.4
	Three-Point	$e_s/L < 0.005$	$<\pm$0.5
Beam Twisting (Table 10)		Minimize θ_s and $\theta_f << 1^o$	---
Bearing Friction (Eqs. 19,20)	Four-Point	Roller bearings which are free to roll.	---
	Three-Point	Roller bearings for outer supports.	---
Contact Stress	Four-Point	$\rho_1/d \geq 7.25\ d/a$	
	Three-Point	$\rho_1/d \geq 29.0\ d/L$	
Wedging Stress (Table 11)	Four-Point	$a/d \geq 5.0$	$<+0.9$
	Three-Point	$L/d \geq 20$	$\leq+0.9$
Beam Overhang		$L_T \geq L + 2d$	---
Contact Point Tangency Shift (Table 12)	1/3 Four-Point	$\rho_1/d \leq 2.0$	$\leq+0.5$
	1/4 Four-Point	$\rho_1/d \leq 1.5$	$\leq+0.7$
	Three-Point	$\rho_1/d \leq 5$	$\leq+0.5$
Corner Chamfer (Table 13)		$b/d = 1.0,\ c/d \leq 0.03$	$\leq$-0.5
		$b/d = 2.0,\ c/d \leq 0.04$	$\leq$-0.5
Corner Radius (Table 13)		$b/d = 1.0,\ r/d \leq 0.04$	$\leq$-0.4
		$b/d = 2.0,\ r/d \leq 0.06$	$\leq$-0.4
Load Readout		Measure ρ accurate to 0.5%	$\leq\pm$0.5%
Specimen Dimension		Measure e_m/d accurate to 0.1%	$\leq\pm$0.3%

STRENGTH AS A FUNCTION OF SPECIMEN DIMENSIONS AND SAMPLE SIZE

General

An additional issue is the question of how many specimens should be broken in a test sequence. Furthermore, it is well known that the size of the specimen can influence the measured strengths. In general, the larger the specimen, the weaker it is likely to be. How can strength results generated with one specimen size be compared to other sizes? These two questions can be addressed by the well-known Weibull analysis.[15]

Many investigators have used the Weibull approach to relate strength levels of various types of specimen configurations either on a stressed volume or surface area basis.[25] The reader is cautioned that confirmation of such an analysis or lack thereof may well depend on a number of factors including the test material. As examples of such correlation and lack of it, Weibull statistical correlation was justified by Davies[25] for reaction-bonded silicon nitride but inappropriate for Lewis' work[26] in alumina fabricated by several processes.

A computer program for statistical evaluation of composite materials, applicable to ceramic materials, is available in Reference 27. This program determines the desirability of a particular probability density function in predicting fracture strength of ranked empirical data. The candidate functions include normal, log normal, and Weibull. Root mean square error results can be tabulated for each functional comparison. The effects of several different statistical ranking schemes can be readily listed in the computer output.

The data mean and standard deviations with corresponding levels of confidence can be included in the printed results. The Weibull parameters, obtained from the maximum likelihood method, and corresponding confidence intervals can be obtained from this program.

Since a Weibull-type analysis is applicable in many instances, resulting formulas for the simple two-parameter system[25,28] to determine the risk of rupture for the four-point and three-point loading systems, are presented below, for the sake of completeness.

It is worth noting that Weibull analyses of strength data require, as input, the idealized tensile stress acting upon a specimen, not the stress at the point of fracture.[25] It is for this reason that strength values are <u>not</u> adjusted in four-point loading for "out of inner span fractures" (which occasionally occur) or for fracture away from the middle bearing in three-point.

Volume Sensitive Material

The Weibull two-parameter volume distribution function for the probability of failure (F) of a uniaxially stressed component is:[15,25]

25. DAVIES, D. G. S. *The Statistical Approach to Engineering Design in Ceramics.* Proc. Br. Ceramics Soc., no. 22, 1973, p. 429-452.
26. LEWIS, D., III. *An Experimental Test of Weibull Scaling Theory.* J. Amer. Cer. Soc., v. 59, no. 11-12, 1976, p. 507-510.
27. NEAL, D. M., and SPRIGIDIGLIOZZI, L. *An Efficient Method for Determining the 'A' and 'B' Design Allowables.* ARO Report 83-2, Proc. of the Twenty-Eighth Conference on the Design of Experiments in Army Research, Development and Testing, 1983.
28. DeSALVO, G. J. *Theory and Structural Design Applications of Weibull Statistics.* Westinghouse Astronuclear Laboratory, WANL-TME-2688, 1970.

$$F = 1 - \exp\left[-\int_V \left(\frac{\sigma}{\sigma_o}\right)^M dV\right] \tag{26}$$

where σ is the tensile stress acting upon an element dV of the component, σ_o is the characteristic strength (a normalizing parameter which has units of stress · volume raised to 1/M), M is the Weibull modulus, and V is the volume of the component. In general, σ is a function of location in the component. Equation (26) is often rewritten for flexure specimens in terms of σ_b and the equivalent volume V_E (the volume of a tensile specimen) which, when subjected to the same stress σ_b, would have the same probability of failure.[25]

$$F = 1 - \exp\left[-\left(\frac{\sigma_b}{\sigma_o}\right)^M V_E\right]. \tag{27}$$

The equivalent volume is a useful quantity since it permits comparison of the mean strengths of two different sized components:*

$$\frac{\sigma_1}{\sigma_2} = \left(\frac{V_{E2}}{V_{E1}}\right)^{1/M} \tag{28}$$

where σ_1 and V_{E1} are the strength and equivalent volume of one component, and σ_2 and V_{E2} are for the other.**

The effective volume of a rectangular beam in four-point flexure is:

$$V_E = V\left(\frac{1}{2(M+1)}\right)\left[1 - \frac{2a}{L}\left(\frac{M}{M+1}\right)\right], \tag{29}$$

where V is the specimen volume inside the outer span (V = bdL). This formulation includes the material between the inner and outer bearings. For the case of 1/4-four-point bending:

$$V_E = V\left[\frac{M+2}{4(M+1)^2}\right]. \tag{30a}$$

For the case of 1/3-point bending:

$$V_E = V\left[\frac{M+3}{6(M+1)^2}\right], \tag{30b}$$

*Or the strengths at the same probability of failure.
**Some assumptions are involved in the above analysis; the reader is directed to Reference 25 for details.

and for a beam stressed in three-point bending:

$$V_E = V\left[\frac{1}{2(M+1)^2}\right]. \tag{30c}$$

M can be determined by a number of different methods (see References 25, 28-30). The accuracy by which M can be determined is discussed later under Weibull Parameter Estimate and Sample Size. Equation 30 shows that a larger volume of material is effectively stressed in four-point as compared to three-point loading. It is for this reason that four-point loading is generally preferred.

Surface Sensitive Material

The Weibull two-parameter surface distribution function for the probability of failure of a uniaxially stressed component is:[15,25]

$$F = 1 - \exp\left[-\int_S \left(\frac{\sigma}{\sigma_o}\right)^M dS\right], \tag{31}$$

where the characteristic strength has units of (stress · area raised to 1/M), M is the Weibull modulus, and integration is performed over the specimen surface, S. If surface flaws predominate, then the effective surface S_E can be used to compare mean strengths* between two components:

$$\frac{\sigma_1}{\sigma_2} = \left(\frac{S_{E2}}{S_{E1}}\right)^{1/M} \tag{32}$$

The effective surface area for a four-point loaded beam is:

$$S_E = \left(\frac{1}{M+1}\right)^2\left\{b\ell(M+1)^2 + [2ab + d\ell](M+1) + 2ad\right\}, \tag{33}$$

and for three-point it is:

$$S_E = \frac{Lb}{M+1} + \frac{Ld}{(M+1)^2} \tag{34}$$

Once again, a greater surface is exposed to high stress in four-point loading as compared to three-point, which is why four-point is preferred.

*Or the strengths at the same probability of failure.

29. McLEAN, A. F., and FISHER, E. A. *Brittle Materials Design, High Temperature Gas Turbine.* Ford Motor Company, Contract DAAG46-71-C-0162, Interim Report, AMMRC CTR 77-20, August 1977.
30. PALUSZNY, A., and WU, W. *Probabilistic Aspects of Designing with Ceramics.* Presented at the 22nd Annual Gas Turbine Conference of A.S.M.E., Philadelphia, Pa., March 27-31, 1977.

Weibull Parameter Estimate and Sample Size

Often, the objective of flexural strength testing is not merely to estimate a mean strength, but to estimate Weibull distribution parameters such as the Weibull modulus M, or the characteristic strength, σ_o. The following section discusses requirements for numbers of specimens in order to obtain reasonable estimates for these parameters.

Flexure tests on hot-pressed silicon nitride material reported by McLean and Baker[31] show the effect of Weibull slope M for specific component reliability. The strength requirement for a specific component reliability was decreased 16% by a reported 20% increase in M from a nominal value of 10, and was increased 27% by a 20% decrease in the slope.

Different techniques will produce somewhat different results, according to McLean and Fisher,[29] when estimating the Weibull parameters. Two statistical methods had been used during preliminary analysis of hot-pressed silicon nitride material strength data, and results indicated that the estimates of the characteristic value σ_o (or scale parameter) were very close while the Weibull slope estimates vary and thus would yield considerable differences in the component strength requirement.

The following is quoted directly from Reference 29 (except to change reference and figure numbers appropriate for this report) because it succinctly addresses the answer to the question of proper sample size: "The exact confidence intervals for the parameters are based on the distributions obtained by Monte Carlo methods presented in Thoman et al.[32] It is not unexpected that the uncertainty in the estimation of a parameter will increase as the sample size decreases. This uncertainty, however, has rarely been quantified. The width of the confidence intervals for the parameters is a measure of the uncertainty and aids in the selection of the sample size of a test. Figures 6 and 7 are drawn from Reference 32 and show the 90% confidence bounds for the Weibull slope and the characteristic value." (Figure 7 differs from that given in Reference 29 in that two additional M values were computed and shown.) "The bounds for the Weibull slope are a function of sample size only, while for the characteristic value they are a function of both the sample size and the Weibull slope. As can be seen from the graphs, the error or uncertainty in estimates from small sample sizes is very large. Important judgements and significant analysis should not be based on small samples. Sample sizes of at least 30 should be used for all but the most preliminary investigations. An uncertainty of ±10% in Weibull slope requires more than 120 samples. This uncertainty is not peculiar to just ceramics, but is intrinsic to the statistical analysis of data, whether that data be material strength or the life of some electronic component. The choice of sample size depends on many factors including the cost and timing of testing and the degree of conservation which is acceptable, but erroneous judgements may be made and unacceptable designs pursued if the sample sizes are too small."

31. McLEAN, A. F., and BAKER, R. R. *Brittle Materials Design, High Temperature Gas Turbine.* Ford Motor Company, Contract DAAG46-71-C-0162, Interim Report, AMMRC CTR 76-31, October 1976.
32. THOMAN, D. R., BAIN, L. J., and ANTLE, C. E. *Inferences on the Parameters of Weibull Distribution.* Technometrics, v. 11, p. 445-460.

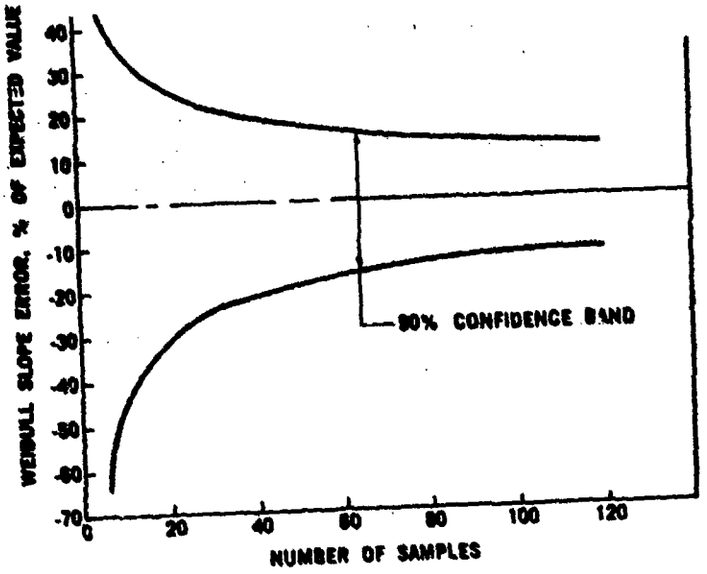

Figure 6. Weibull slope error versus sample size.

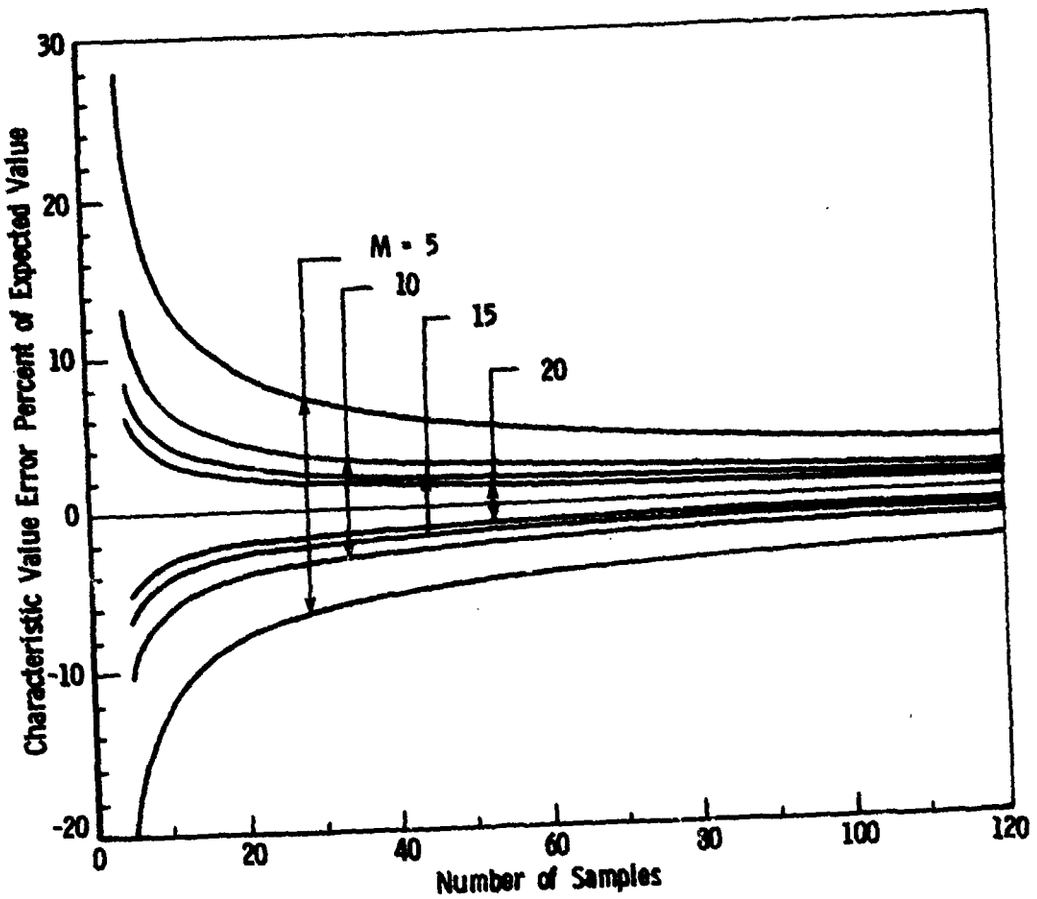

Figure 7. Characteristic value error versus sample size - 90% confidence bands.

LOADING SPEED

It is well known that speed of loading will often influence the failure stress of structural ceramic beams. The source of the sensitivity is stress corrosion phenomena, particularly in the presence of water or water vapor. In general, the slower the speed of loading, the greater the opportunity for stress corrosion phenomena to weaken the specimen. Thus, fast loading speeds are usually used in strength tests.

Most universal testing machines used for flexure testing are constant displacement rate machines, so it is convenient to specify strain rates. The strain rate for a linearly elastic material is defined as:

$$\dot{\varepsilon} = (\sigma_b/E)/t \ , \tag{35}$$

where t is the time of the applied load; but since the speed of loading is s = y/t, then

$$\dot{\varepsilon} = \left(\frac{\sigma_b}{E}\right)\left(\frac{s}{y}\right), \tag{36}$$

where y is the deflection of the beam and s the constant speed of the testing machine. This assumes that all of the machine's motion is transmitted to the specimen (i.e., the machine is perfectly 'hard'). The deflection of the inner load bearings of a four-point loaded beam is:

$$y = \frac{p^2a}{6EI}(3L - 4a) \ . \tag{37}$$

Substitution of y into Equation 36 and recognizing that $\sigma_b = Pad/2I$ gives:

$$\dot{\varepsilon} = \frac{3Sd}{a(3L - 4a)} \ . \tag{38}$$

For a 1/4-four-point beam:

$$\dot{\varepsilon} = \frac{6dS}{L^2} \ . \tag{39}$$

For a 1/3-point beam:

$$\dot{\varepsilon} = \frac{27dS}{5L^2} \ . \tag{40}$$

Using the same approach as above, we obtain the strain rate for three-point beams:

$$\dot{\varepsilon} = \frac{6dS}{L^2} \tag{41}$$

An alternative approach to designating the loading speed is the stressing rate:

$$\dot{\sigma} = \dot{\varepsilon}E \tag{42}$$

which is valid for the case of a linearly elastic material. Equations 38 to 41 can be substituted into Equation 42 if stressing rates are specified.

Finally, if the time per test is the limiting concern, then the following is applicable:

$$t = \frac{\sigma_b}{\dot{\sigma}} , \tag{43}$$

and Equations 38-42 can be used along with the projected bend strength to solve for t.

CONCLUSIONS

A variety of sources can lead to errors in determining the flexure strength when using simple beam theory equations. These sources include assumptions involving simple beam theory and external influences pertaining to the load application. Providing that the beam is homogeneous and isotropic, and deflections are relatively small, then the major sources of error are from external sources. In particular, the most serious errors arise from load bearing friction, beam twisting, and load bearing mislocation. Other errors, such as contact point tangency shift, wedging stresses, neglecting corner chamfers, and load readout errors cannot be neglected either. Table 14 lists all of the potential error sources identified in this report and makes specific recommendations for specimen and fixture geometries and tolerances. The bases for the recommendations are that they be practical, that they limit the individual errors to approximately one half percent, and that the sum of the errors be less than a few percent.

Requirements for a minimum number of recommended specimens (30) are presented in the context of the Weibull two-parameter analysis. This analysis is one of the simplest possible, and the reader is cautioned that numerous assumptions are entailed in its use. Even if a more complex function appears to have better applicability than a Weibull analysis, the requirement for 30 or more specimens should likely remain valid.

For convenience, a brief discussion of converting strength of one size specimen to another is included. Again, since this analysis is based upon a Weibull two-parameter approach, the reader is cautioned that numerous assumptions apply and that more sophisticated analyses may have to be used.

A section on loading speed is also included for convenience to permit quick assessment of optimum universal testing machine speeds.

TABULATIONS OF ERRORS IN CALCULATING FLEXURE STRESS

Unless otherwise stated, the percent error is determined throughout the text as $\bar{\epsilon} = [(\sigma_b - \sigma_x)/\sigma_x]100$; where $\sigma_b = 6M/bd^2$ and σ_x is more nearly the true bending stress. Thus a negative error indicates the simple beam formulas 1a and 1b underestimate the true stress; a positive error is an overestimate.

ACKNOWLEDGEMENT

The authors wish to recognize the support and encouragement extended by Dr. R. Chait, Chief, Materials Integrity and Testing Technology Division, and the assistance of Mr. T. Stefanick who computer programmed the error analyses.

REFERENCES

1. BARATTA, F. I. *Requirements for Flexure Testing of Brittle Materials.* U. S. Army Materials and Mechanics Research Center, AMMRC TR 82-20, April 1982, ADA 113937.
2. U. S. ARMY MIL-STD-1942 (MR). *Flexure Testing of High Performance Ceramics at Ambient Temperature.* November 1983.
3. TIMOSHENKO, S., and GOODIER, J. N. *Theory of Elasticity.* 2nd Ed., McGraw-Hill Book Co., Inc., New York, 1951.
4. TIMOSHENKO, S. *Strength of Materials.* 3rd Ed., D. Van Nostrand Co., Inc., N.Y., 1958, and Part II, 2nd Ed., D. Van Nostrand Co., Inc., N.Y. 1941.
5. CHAMLIS, C. C. *Analysis of Three-Point-Bend Test for Materials with Unequal Tension and Compressive Properties.* NASA TN D7572, March 1974.
6. LEKHNITSKII, S. G. *Theory of Elasticity of an Anisotropic Elastic Body.* Holden-Day Series in Mathematical Physics, J. L. Brandstatter, ed., 1963, p. 204.
7. TIMOSHENKO, S. *Letter to the Editor.* Mechanical Engineering, v. 45, no. 4, April 1923, p. 259-260.
8. BARATTA, F. I. *When is a Beam a Plate?* J. Amer. Cer. Soc., v. 64, no. 5, 1981, p. c-86.
9. ASHWELL, D. G. *The Anticlastic Curvature of Rectangular Beams and Plates.* J. Roy., Aero. Soc., v. 54, 1950, p. 708-715.
10. WEST, D. C. *Flexure Testing of Plastics.* Exp. Mech., v. 21, no. 2, July 1964.
11. RITTER, J. E., and WILSON, W. R. D. *Friction Effects in Four-Point Bending.* ASLE Transactions, v. 18, no. 2, p. 130-134, presented at the 29th Annual Meeting, April 28-May 2, 1974.
12. TIMOSHENKO, S., and GERE, J. M. *Theory of Elastic Stability.* McGraw-Hill Book Co., Inc., New York, 1961.
13. RUDNICK, H., MARSCHALL, C. W., DUCKWORTH, W. H., and ENRICK, B. R. *The Evaluation and Interpretation of Mechanical Properties of Brittle Materials.* AFME TR 67-316, April 1968.
14. OH, H. L., and FINNIE, I. *On the Location of Fracture in Brittle Solids - I, Due to Static Loading.* Int. J. of Fracture Mechanics, v. 6, no. 3, September 1970, p. 287-300.
15. WEIBULL, W. *Statistical Theory of Strength of Materials.* Royal Swedish Institute for Engineering Res., Proc. no. 151, 1939, p. 1-45.
16. HOAGLAND, R. G., MARSCHALL, C. W., and DUCKWORTH, W. H. *Reduction of Errors in Ceramic Bend Tests.* J. Amer. Cer. Soc., v. 59, no. 5-6, May-June 1976, p. 189-192.
17. JAYATILAKA, A. DeS. *Fracture of Engineering Brittle Materials.* Applied Science Publishers, LTD, London, 1979, p. 187.
18. DUCKWORTH, W. H., et al. *Mechanical-Property Tests on Ceramic Bodies.* WADC TR 52-67, March 1952, p. 67-70.
19. NEWNHAM, R. C. *Strength Tests for Brittle Materials.* Proc. of the British Cer. Soc., no. 25, May 1975, p. 281-293.
20. WEIL, N. A. *Studies of Brittle Behaviour of Ceramic Materials.* ASD TR 61-628, Part II, April 1962, p. 38-42.
21. VON KARMAN, T., and SEEWALD, F. Aihandl Aerodynam, Inst. Tech. Hochschule, 1946, p. 256.
22. WESTWATER, J. W. *Flexure Testing of Plastic Materials.* Proc. ASTM, v. 49, 1949.
23. RICE, R. W. *Machining of Ceramics.* Proc. of the Second Army Materials Technology Conference - Ceramics for High Performance Applications, J. J. Burke, A. E. Gorum, and R. N. Katz, ed., Brook Hill Publishing Company, Chestnut Hill, Massachusetts, 1974.
24. RICE, R. W. *The Effect of Grinding Direction on the Strength of Ceramics.* The Science of Ceramics Machining and Surface Finishing, S. J. Scheider and R. W. Rice, ed., NBS Special Publication 348, Washington, DC, Government Printing Office (SD Catalog No. 13.10:348), 1972, p. 365-376.
25. DAVIES, D. G. S. *The Statistical Approach to Engineering Design in Ceramics.* Proc. Br. Ceramics Soc., no. 22, 1973, p. 429-452.
26. LEWIS, D., III. *An Experimental Test of Weibull Scaling Theory.* J. Amer. Cer. Soc., v. 59, no. 11-12, 1976, p. 507-510.
27. NEAL, D. M., and SPRIGIDIGLIOZZI, L. *An Efficient Method for Determining the 'A' and 'B' Design Allowables.* ARO Report 83-2, Proc. of the Twenty-Eighth Conference on the Design of Experiments in Army Research, Development and Testing, 1983.
28. DeSALVO, G. J. *Theory and Structural Design Applications of Weibull Statistics.* Westinghouse Astronuclear Laboratory, WANL-TME-2688, 1970.
29. McLEAN, A. F., and FISHER, E. A. *Brittle Materials Design, High Temperature Gas Turbine.* Ford Motor Company, Contract DAAG46-71-C-0162, Interim Report, AMMRC CTR 77-20, August 1977.
30. PALUSZNY, A., and WU, W. *Probabilistic Aspects of Designing with Ceramics.* Presented at the 22nd Annual Gas Turbine Conference of A.S.M.E., Philadelphia, Pa., March 27-31, 1977.
31. McLEAN, A. F., and BAKER, R. R. *Brittle Materials Design, High Temperature Gas Turbine.* Ford Motor Company, Contract DAAG46-71-C-0162, Interim Report, AMMRC CTR 76-31, October 1976.
32. THOMAN, D. R., BAIN, L. J., and ANTLE, C. E. *Inferences on the Parameters of Weibull Distribution.* Technometrics, v. 11, p. 445-460.

APPENDIX A. ANTICLASTIC CURVATURE

When a beam is bent by a moment, it produces a curvature ρ along its longitudinal axis; there is also curvature present in the transverse or lateral direction. This moment is defined by orthodox theory as

$$M_b = (EI/\rho)\beta \tag{A-1}$$

where β is a parameter representing the effect of restraint of anticlastic curvature after Ashwell.[9] Since

$$\sigma_x = M_b c/I = (EI/\rho I)y\beta$$

then

$$\sigma_x = (Ey/\rho)\beta \tag{A-2}$$

where y is the distance from the neutral axis.

The β for simple beam theory will equal 1.0 and if the beam width to depth is great, i.e., $b/d^* \to \infty$, the beam can be considered as a plate so that $\beta \to 1/(1-\nu^2)$. It is worthwhile to know the intermediate values of β such that the effect of restraint of anticlastic curvature on the error can be ascertained when assuming simple beam theory ($\beta = 1.0$) is valid.

Ashwell[9] has determined β as a function of Poisson's ratio, beam width, depth, and neutral axis curvature by accounting for anticlastic curvature and treating the structure as a beam on an elastic foundation. The function β and related terms are repeated here in the following:

$$\beta = \frac{1}{1-\nu^2} + \frac{3}{2\,\gamma b} f(\gamma b) - \frac{2\sqrt{3}\,\nu}{\gamma b\sqrt{1-\nu^2}} F(\gamma b) \tag{A-3}$$

where

$$\gamma = \sqrt[4]{\frac{3(1-\nu^2)}{d^2\rho^2}},$$

$$f(\gamma b) = 2(B^2+C^2)[\sinh(\gamma b) + \sin(\gamma b)]$$
$$+ (B^2-C^2+2BC)\cosh(\gamma b)\sin(\gamma b)$$
$$+ (B^2-C^2-2BC)\sinh(\gamma b)\cos(\gamma b)$$
$$+ 2(B^2-C^2)(\gamma b),$$

$$F(\gamma b) = (B+C)\sinh(\gamma b/2)\cos(\gamma b/2)$$
$$- (B-C)\cosh(\gamma b/2)\sin(\gamma b/2),$$

*To be more exact, $b^2/\rho d \to \infty$.

$$B = \frac{\nu}{\sqrt{3(1-\nu^2)}}\left(\frac{\sinh(\gamma b/2)\cos(\gamma b/2) - \cosh(\gamma b/2)\sin(\gamma b/2)}{\sinh(\gamma b) + \sin(\gamma b)}\right), \text{ and}$$

$$C = \frac{\nu}{\sqrt{3(1-\nu^2)}}\left(\frac{\sinh(\gamma b/2)\cos(\gamma b/2) + \cosh(\gamma b/2)\sin(\gamma b/2)}{\sinh(\gamma b) + \sin(\gamma b)}\right).$$

The calculations performed for Table 3 in the text were accomplished in the following manner:

Since

$$\gamma b = b\sqrt[4]{\frac{3(1-\nu^2)}{d^2\rho^2}}, \text{ and } \rho = (E/\sigma)y\beta, \text{ then substituting into the above,}$$

allowing $y = d/2$, $E/\sigma = E/\sigma_b = 1 \times 10^3$, and $\nu = 0.25$ for ceramic materials, we have;

$$\gamma b = \frac{57.915 \times 10^{-3}\,(b/d)}{\sqrt{\beta}}. \qquad \text{(A-4)}$$

By programming (A-3) and *prescribing* b/d, but first allowing $\beta=1.0$, then iterating in the computer through (A-4), the relationship between b/d and β was obtained. Once this relationship is known, the percent error, defined as $[(1-\beta)/\beta]100$, as a function of b/d is realized. These errors are given in Table 3 as a function of b/d with $E/\sigma_b = 1000$ and $\nu = 0.25$.

APPENDIX B. LOAD MISLOCATION ERROR, LOADING HEAD RIGIDLY ATTACHED

Four-Point Loading

Consider the usual flexure testing setup where the loading head is rigidly attached to a testing machine, schematically shown in Figure 1b and idealized in Figure 1c. The upper loading head, where the inner span ℓ is fixed, can only translate in the vertical direction, and the lower support fixture, where the outer span L is fixed, can be located with reference to the loading head. The slope and deflection equations between points AB, BC, and CD are as follows:

$$\left.\begin{aligned} EI\,(dy_{AB}/dx) &= (P_1x^2/2) + c_1 \\ EI\,y_{AB} &= (P_1x^3/6) + c_1x + c_2 \end{aligned}\right\} \qquad \text{(B-1a)}$$

$$\left.\begin{aligned} EI\,(dy_{BC}/dx) &= (P_1-P_2)(x^2/2) + P_2a_1x + c_3 \\ EI\,y_{BC} &= (P_1-P_2)(x^3/6) + (P_2a_1x^2/2) + c_3x + c_4 \end{aligned}\right\} \qquad \text{(B-1b)}$$

and

$$\left.\begin{aligned} EI\,(dy_{CD}/dx) &= (P_1-P_2-P_3)(x^2/2) + P_2a_1x + P_3\,(a_1+\ell)\,x + c_5 \\ EI\,y_{CD} &= (P_1-P_2-P_3)(x^3/6) + (P_2a_1x^2/2) + P_3\,(a_1+\ell)(x^2/2) + c_5x + c_6 \end{aligned}\right\} \qquad \text{(B-1c)}$$

where P_1, P_2, P_3, and P_4 are the loads, x and y are defined as shown in Figure 1, E is the Young's modulus of the material, and I is the moment of inertia of the cross section of the beam.

Through the use of the various boundary conditions the constants are determined to be:

$$c_1 = -1/6 \{P_1(L^2-a_2^2) + (P_2/L)\ [(a_1-L)^3 + (\ell+a_2)a_2^2]\}$$

$$c_2 = 0$$

$$c_3 = -1/6 \{P_1(L^2-a_2^2) + (P_2/L)\ [3a_1^2L - (a_2+\ell)^3 + (\ell+a_2)a_2^2]\}$$

$$c_4 = P_2a_1^3/6$$

$$c_5 = -1/6 \{P_1L^2 + (P_2/L)\ [a_1^3+3a_1L^2-L^3] + (P_3/L)\ [(a_1+\ell)^3 + 3(a_1+\ell)\ L^2-L^3]\}$$

$$c_6 = P_3[(a_1+\ell)^3/6] + (P_2a_1^3/6).$$

In order to determine the distribution of loading between the vertical loads P_1, P_2, P_3, and P_4, the final condition of equal deflection must be enforced at locations B and C (see Figure 1b), which is

$$(y_{BC})_{x=a_1} = (y_{BC})_{x=a_1+\ell}.$$

Enforcing the above condition in the second part of Equation B-1b results in

$$P_1/P_2 = -(\ell/L)^2 \left\{ \frac{\ell/L - (1-a_1/L)(2-\ell/L-2a_1/L)}{(a_1/L)^3 - (a_1/L+\ell/L)^3 + \{1 - [1-(\ell/L)-a_1/L]^2\}(\ell/L)} \right\}. \quad \text{(B-2)}$$

Utilizing force and moment equilibrium, a further relationship between all four forces is obtained and given in the following:

$$P_4/P_3 = \frac{(P_1/P_2)(a_1/L) + (P_1/P_2-1)\ell/L}{(P_1/P_2) - 1 + a_1/L} \quad \text{and} \quad P_3/P_2 = \frac{P_1/P_2 + a_1/L - 1}{1 - a_1/L - \ell/L}. \quad \text{(B-3)}$$

The ratio of the stress at x (σ_x) to the bending stress (σ_b) from Reference 16 or Equation 9 in the text, where it is assumed that $a_1 \neq a_2$, is:

$$\sigma_x/\sigma_b = \left[\frac{P_1}{\frac{P_2+P_3}{2}} \right] \frac{x_1}{a} \quad \text{(B-4)}$$

where a is the value at a_1 with perfect load location and x_1 is defined as shown in Figure 1c.

By manipulation of (B-2) and (B-3), the factor $P_1/(P_2+P_3)$ in (B-4) can be put into terms of a_1/L and ℓ/L. This was accomplished and the results are shown in the following equation:

$$\sigma_x/\sigma_b = \frac{[(a_1/L)/(a/L)](1 - a_1/L - \ell/L)[(\ell/L)(2 - a_1/L) - 2(1 - a_1/L)^2]}{3(a_1/L)(1 - \ell/L - a_1/L) - (1 - \ell/L)^2} \quad \text{(B-5)}$$

By defining the eccentricity of loading as $e/L = a_1/L - a/L$, Equation B-5 becomes:

$$\sigma_x/\sigma_b = \frac{[(e/L + a/L)/(a/L)][1-(e/L + a/L)- \ell/L]\{(\ell/L)[2-(e/L + a/L)] - 2[1-(e/L + a/L)]^2\}}{3(e/L + a/L)[1 - \ell/L - (e/L + a/L)]-(1- \ell/L)^2} \quad \text{(B-6)}$$

Calculations of σ_x/σ_b were obtained for $\ell/L = 1/3$ as well as $\ell/L = 1/2$, by allowing e/L to take on negative values only in Equation B-6. Only negative values were considered because beam failure will occur due to a realistically larger moment than idealized when ignoring eccentricity. These error calculations, although determined by allowing $e/L < 0$ in Equation B-6, are indicated as $\pm e/L$ in Table 5 for $\ell/L = 1/3$ and Table 6 for $\ell/L = 1/2$. This simply indicates that the location of the maximum moment or stress is at $x_1 = a_1$ when $e/L < 0$ and at $x_1 = a_1 + \ell$ when $e/L > 0$.

The reader is cautioned that for each value of ℓ/L there exists a set of limits on (B-2), (B-3), and (B-5). That is, a_1 can be such that either P_2 or P_3 can equal zero, because $(Y_{BC})_{x=a_1} \neq (Y_{BC})_{x=a_1+\ell}$ and the system changes from four-point to an eccentric three-point loading. The limiting values can be determined by allowing $P_2 = 0$ in Equation B-2.

APPENDIX C. BEAM TWISTING

If line loads are nonuniform or nonparallel between pairs of load contacts, or if the cross section of the specimen is skewed along its length, as shown in Figure 3, a net torque will result. The addition of torque gives rise to a maximum principal stress due to bending and torsional stresses.[13,16] Failure assumed to be caused only by bending stress will yield an error. Two cases are considered: Case I - Failure occurs prior to specimen realignment in the bend fixture (bottoming), and Case II - Failure occurs at or after bottoming.

Case I

Recalling that the bending stress for a loaded beam is

$$\sigma_x = \sigma_b = 6M_b/bd^2 \quad \text{(C-1)}$$

where M_b is the measured bending moment at failure; for a four-point loaded beam $M_b = Pa$, and for a three-point loaded beam $M_b = PL/4$.

The maximum shear stress due to torsion of a rectangular beam is[3]

$$\tau_{xz} = T_b/k_2bd^2 \quad \text{(C-2)}$$

where T_b is the torque and equal to Pb for four-point bending and Pb/2 for three-point bending, and k_2 is a numerical factor obtained from Reference 3 and is given in Table 9. This peak shear stress occurs at the specimen surface at the midpoint of the long edge (dimension b).

Prior to bottoming, the normal stress is

$$\sigma_n = (\sigma_z/2)(1-\cos 2\theta) + (\sigma_x/2)(1+\cos 2\theta) + \tau_{xz}\sin 2\theta, \qquad \text{(C-3)}$$

on a plane whose normal is in the xz plane and is inclined at an angle θ to the x axis. Since we shall assume a plane strain condition, i.e., $\varepsilon_z = 0$, then

$$\varepsilon_z = 0 = (1/E)(\sigma_z - \nu\sigma_x) \text{ or } \sigma_z = \nu\sigma_x = \nu\sigma_b$$

since $\sigma_y = 0$ at the free surface. From Equation C-3:

$$\sigma_n = (\sigma_b/2)[(1+\nu) + (1-\nu)\cos 2\theta] + \tau_{xz}\sin 2\theta. \qquad \text{(C-4)}$$

Now σ_n is maximum when

$$\tan 2\theta^* = 2\tau_{xz}/(\sigma_x - \sigma_z);$$

but since

$$\sigma_z = \nu\sigma_x$$

then

$$\tan 2\theta^* = 2\tau_{xz}/(1-\nu)\sigma_b \qquad \text{(C-5)}$$

where θ^* is the angle of a plane inclined to the axis at which principal stress is a maximum. Substitution of (C-1) and (C-2) into (C-5) for the condition prior to bottoming gives:

$$\tan 2\theta^* = (T_b/M_b)/[3(1-\nu)k_2], \qquad \text{(C-6)}$$

$$\sin 2\theta^* = (T_b/M_b)/[(T_b/M_b)^2 + (3k_2)^2(1-\nu)^2]^{1/2}, \qquad \text{(C-7)}$$

and

$$\cos 2\theta^* = [3k_2(1-\nu)]/[(T_b/M_b)^2 + (3k_2)^2(1-\nu)^2]^{1/2}. \qquad \text{(C-8)}$$

From Equations C-1 and C-2

$$\tau_{xz} = (\sigma_b/2)[(T_b/M_b)/3k_2], \qquad \text{(C-9)}$$

and by substitution of the above relationships into (C-4) with some algebraic manipulation, we obtain:

$$\sigma_{n_{max}} = (\sigma_b/2)\left\{(1+\nu) + (1/3k_2)[(T_b/M_b)^2 + 9(1-\nu)^2k_2^2]^{1/2}\right\} \qquad \text{(C-10)}$$

prior to bottoming. The shear stress due to torsion can be related to the twist angle[3] of the beam through the following relationship:

$$\tau_{xz} = (k_1/k_2)Gd[(\phi_s/L_T) + (\phi_F/\ell')] \qquad \text{(C-11)}$$

where ϕ_s is the twist angle along the length of the specimen (see Figure 3b), ϕ_F is the twist angle between a pair of load and contact points relative to ϕ_s (see Figure 3c), ℓ' is equal to either "a" for four-point beam systems or L/2 for three-point beam systems, k_1 is another numerical factor[3] given in Table 9, and $G = E/2(1+\nu)$, the shear modulus of the material.

Equation (C-2) can be equated to (C-11) and thus we obtain:

$$T_{b_e} = [k_1 E/2(1+\nu)]bd^2[(d/L_T)\phi_s + (d/\ell')\phi_F] \qquad (C\text{-}12)$$

where T_{b_e} is the torque when bottoming occurs. Thus, in order for (C-10) to be applicable, T_b must be less than T_{b_e}, and since $T_b = (b/\ell')M_b$ and from (C-1) and (C-12):

$$T_{b_e}/T_b = [3k_1 E/\sigma_b(1+\nu)(b/\ell')]bd^2[(d/L_T)\phi_s + (d/\ell')\phi_F] \geq 1.0, \text{ or}$$

$$n = (\ell'/b)[3k_1(E/\sigma_b)/(1+\nu)][(d/L_T)\phi_s + (d/\ell')\phi_F] > 1.0 \qquad (C\text{-}13)$$

where σ_b is the bending stress at failure according to (C-1).

Note that $T_b/M_b = b/\ell'$ and for four-point loading $\ell' = a$; for three-point loading $\ell' = L/2$, thus (C-10) becomes:

$$\sigma_{n_{max}} = (\sigma_b/2)\left\{(1+\nu) + (1/3k_2)[(b/\ell')^2 + 9(1-\nu)^2 k_2^2]^{1/2}\right\} \qquad (C\text{-}14)$$

with $n \geq 1.0$.

Case II

If, however, $n < 1.0$ then bottoming occurs prior to or at failure and the following analysis is applicable.

Equations (C-4) and (C-5) are still appropriate but the shear stress is

$$\tau_{xz} = T_{b_e}/k_2 bd^2. \qquad (C\text{-}15)$$

Substitution of τ from the above and σ_b from (C-1) into (C-5) gives

$$\tan 2\theta^* = (T_{b_e}/M_b)/3(1-\nu)k_2,$$

but from (C-13) $T_{b_e} = nT_b$ and thus:

$$\tan 2\theta^* = (nT_b/M_b)/3(1-\nu)k_2. \qquad (C\text{-}16)$$

As in Case I, using a like procedure we determine $\sigma_{n_{max}}$ to be:

$$\sigma_{n_{max}} = (\sigma_b/2)\left\{(1+\nu) + (1/3k_2)[n^2(T_b/M_b)^2 + 9(1-\nu)^2k_2^2]^{1/2}\right\} \quad \text{(C-17)}$$

with

$$n = \left(\frac{\ell'}{b}\right)[3k_1(E/\sigma_b)/(1+\nu)][(d/L_T)\phi_s + (d/\ell')\phi_p] \leq 1.0. \quad \text{(C-18)}$$

Equation (C-17) is applicable to both systems since $(T_b/M_b) = b/\ell' = b/a$ for the four-point beam bending system, and $(T_b/M_b) = 2b/L$ for the three-point system. Thus (C-17) becomes

$$\sigma_{n_{max}} = (\sigma_b/2)\left\{(1+\nu) + (1/3k_2)[(nb/\ell')^2 + 9(1-\nu)^2k_2^2]^{1/2}\right\}. \quad \text{(C-19)}$$

Notice when n = 1, (C-19) reduces to (C-14).

Finally, the percent error is defined as:

$$\bar{\varepsilon} = [(\sigma_b - \sigma_{n_{max}})/\sigma_{n_{max}}]100. \quad \text{(C-20)}$$

Errors were calculated in accordance with (C-20), with $\nu = 0.25$ for Case I (n = 0.20, 0.40, 0.60, and 0.80) and Case II (n = 1.0).

If, instead of plane strain ($\varepsilon_z = 0$), it had been assumed that a plane stress ($\sigma_z = 0$) condition applied, then the maximum principal stresses are given by the same Equations C-10, C-14, C-17, and C-19, but with Poisson's ration $\nu = 0$. Equations C-12, C-13, and C-18 are unchanged however, since $G = E/2(1+\nu)$. The plane strain analyses gives a higher error estimate, but the plane stress condition is closer to the actual case since lateral constraint is negligible.

APPENDIX D. WEDGING STRESSES

We allow the stress in the x direction in Figures 1 and 2 to be

$$\sigma_x = \sigma_b + (2P/bd)\beta_T, \quad \text{(D-1)}$$

where σ_b is the bending stress, i.e., $\sigma_b = (6M_x/bd^2)$, and 2P/bd is the local stress, i.e., the so-called wedging stress, and β_T is a numerical factor dependent on the normalized distance $x'/(d/2)$ on either side of the applied load point.[3]

For convenience the value of β_T at the tensile side of the beam as a function of x'/d is given in Table D-1.

The percent error is defined as:

$$\bar{\varepsilon} = [(\sigma_b - \sigma_x)/\sigma_x]100, \quad \text{(D-2)}$$

and substitution of (D-1) into the above equation gives

$$\bar{\varepsilon} = \left\{-\beta_T/[(\sigma_b/2P/bd)+\beta_T]\right\} 100. \qquad \text{(D-3)}$$

Since $\sigma_b = 6M_x/bd^2$, then (D-3) becomes:

$$\bar{\varepsilon} = \left\{-\beta_T/(3M_x/Pd+\beta_T)\right\} 100. \qquad \text{(D-4)}$$

For a four-point loaded beam the bending moment is constant, i.e., $M_x = Pa$, and thus equation (D-4) becomes:

$$\bar{\varepsilon} = \left\{-\beta_T/[(3a/d)+\beta_T]\right\} 100. \qquad \text{(D-5)}$$

From Table D-1 and Equation D-5 above, it is seen that the error is dependent on β_T or the fracture location, which is the normalized distance x'/d. These errors have been computed for the four-point loaded beam and presented in Table 11a.

For the three-point loaded beam, (D-4) is still applicable, but recalling that $M_x = P/2[(L/2)-x']$ and substituting M_x into (D-4) gives:

$$\bar{\varepsilon} = \left\{-\beta_T/\left(\tfrac{3}{4}(L/d)-\tfrac{3}{2}(x'/d)+\beta_T\right)\right\} 100 \text{ for } x' < L/2. \qquad \text{(D-6)}$$

Again, as can be seen by (D-6), the percent error is dependent upon β_T and the normalized fracture location. These percent errors are given in Table 11b.

Table D-1. WEDGING PARAMETER β_T

$\pm x'/d$	β_T
0	-0.1332
0.125	+0.0137
0.250	+0.0868
0.375	+0.0640
0.500	+0.0421
0.750	+0.0220
1.000	+0.0095
1.500	+0.00075

APPENDIX E. CONTACT POINT TANGENCY SHIFT

Consider the four-point loaded beam shown in Figure 4. The original span "a" is seen to decrease by the amount (h_1+h_2) due to rolling or slipping of the beam on its support and load points. The beam fulfills the condition:*

*It is realized that a change in the resultant load vectors must give rise to horizontal reactions; but it is assumed that this effect is small, and is thus ignored.

$$dy^2/dx^2 = M_x/EI. \qquad \text{(E-1)}$$

The moments are defined as:

$$M_x = P(x-h_1), \qquad 0 \le x \le (a-h_2)$$

$$M_x = P[a-(h_1+h_2)], \quad (a-h_2) \le x \le L-(a-h_2).$$

The slope equations are

$$EI(dy/dx) = P[(x^2/2)-h_1x] + C_1, \quad 0 \le x \le (a-h_1), \text{ and} \qquad \text{(E-2)}$$

$$EI(dy/dx) = P[a-(h_1+h_2)]x + C_2, \quad (a-h_2) \le x \le L-(a-h_2). \qquad \text{(E-3)}$$

Now when $x = a-h_2$,

$$C_1 + P\left\{[(a-h_2)^2/2] - (a-h_2)h_1\right\} = P[a-(h_1+h_2)](a-h_2) + C_2, \text{ or}$$

$$C_2-C_1 = -(P/2)(a-h_2)^2. \qquad \text{(E-4)}$$

Note also that when $x = L/2$ and $dy/dx = 0$ in (E-3),

$$C_2 = -P[a-(h_1+h_2)]L/2. \qquad \text{(E-5)}$$

After substitution of C_2 into (E-4) we obtain:

$$C_1 = (P/2)\left\{(a-h_2)^2 - L[a-(h_1+h_2)]\right\}. \qquad \text{(E-6)}$$

Substitution of these constants into the appropriate slope equations gives:

$$EI(dy/dx) = P[(x^2/2)-h_1x] + (P/2)\left\{(a-h_2)^2 - L[a-(h_1+h_2)]\right\} \qquad \text{(E-7)}$$

with $0 \le x \le (a-h_2)$, and

$$EI(dy/dx) = P[a-(h_1+h_2)][x-(L/2)], \qquad \text{(E-8)}$$

with $(a-h_2) \le x \le L-(a-h_2)$.

Now when x = [illegible] from the geometry $dy/dx = -h_1/\sqrt{\rho_1^2-h_1^2} \approx -h_1/\rho_1$ and when $x = a-h_2$, $dy/dx = -h_2/\sqrt{\rho_2^2-h_2^2} \approx -h_2/\rho_2$. The above relationships are used with (E-7) and (E-8) and we obtain:

$$(\rho_1/d) = \frac{(h_1/a)(E/\sigma_b)}{(h_1/a)^2 - (\text{[illegible]}/a)^2 + (L/a)[1-(h_1/a + h_2/a)]} \qquad \text{(E-9)}$$

and

$$1-(h_2/a) = (1/2)\left\{[(L/2a) + (h_1/a) + A_2] - \sqrt{[(L/2a) + (h_1/a) + A_2]^2 - 4[(h_1/a)(L/2a) + A_2]}\right\} \quad \text{(E-10)}$$

where $A_2 = (E/2\sigma_b)/(\rho_2/d)$.

Note that for the three-point loading case $h_2 = 0$, $L/a = 2$, and $P \rightarrow P/2$ and (E-9) reduces to:

$$\rho_1/d = [2(h_1/L)(E/\sigma_b)]/[(2h_1/L)-1]^2, \quad \text{(E-11)}$$

and the region of validity of (E-10) vanishes.

The percent error is defined as:

$$\bar{\varepsilon} = [(\sigma_b-\sigma_x)/\sigma_x]100 = [(M_b-M_x)/M_x]100, \text{ or}$$

$$\bar{\varepsilon} = \left\{[(h_1/a) + (h_2/a)]/[1 - (h_1/a) - (h_2/a)]\right\}100 \quad \text{(E-12)}$$

for four-point loading and

$$\bar{\varepsilon} = \left\{(2h_1/L)/[1 - (2h_1/L)]\right\}100 \quad \text{(E-13)}$$

for three-point loading.

Calculations were performed by the following procedure. It was assumed that $E/\sigma_b = 1 \times 10^3$, and thus $A_2 = (1 \times 10^3)/(\rho_2/d)$; then for the 1/3- and 1/4-four-point loading case $a/L = 1/3$ and $1/4$, numerical values were assigned to ρ_2/d and h_1/a and then h_2/a was determined from (E-10). Those numerical values of h_1/a and corresponding h_2/a were substituted into (E-9) to determine ρ_1/d. This same procedure was used for the three-point loading case with $h_2 = 0$ and $L/a = 2$. Once the parameters h_1/a, h_2/a, ρ_2/d and ρ_1/d are known, percent errors according to (E-12) for the four-point loading case and (E-13) for the three-point loading case can be determined. Such errors are given in Tables 12a-c.

APPENDIX F. ERROR DUE TO NEGLECTING CHANGE IN MOMENT OF INERTIA CAUSED BY CORNER RADII OR CHAMFERS

Corner Radius

Consider Figure 5a, which shows the cross section of a rectangular beam with corner radii r. The true moment of inertia $(I_{xx})_r$ about the centroidal or neutral axis x-x is:

$$(I_{xx})_r = b(d-2r)^3/12 + (b-2r)r^3/6 + (1/2)(b-2r)(d-r)^2r + 4r^4(\pi/16 - 4/9\pi) + \pi r^2[d/2 - r(1 - 4/3\pi)]^2. \quad \text{(F-1)}$$

Most investigators, however, will neglect the loss of inertia when calculating the bending stress due to corner radii and assume that $I_b = bd^3/12$, and the error in stress becomes

$$\left\{\frac{(I_{xx})_r}{I_b} - 1\right\} 100$$

$$\bar{\epsilon} = \left(\frac{\left[b(d-2r)^3 + 2(b-2r)r^3 + 6(b-2r)(d-r)r^2 + 48r^4\left(\frac{\pi}{16} - \frac{4}{9\pi}\right) + 12\pi r^2 \left\{\frac{d}{2} - r\left(1 - \frac{4}{3\pi}\right)\right\}^2 \right]}{bd^3} - 1.0 \right) \times 100 \qquad \text{(F-2)}$$

45^0 Chamfer

Now consider Figure 5b, which shows a rectangular beam with 45^0 corner chamfer c. The true moment of inertia $(I_{xx})_c$ about the x-x axis is:

$$(I_{xx})_c = (bd^3/12) - (c^2/9)\left[c^2 + (1/2)(3d-2c)^2\right] , \qquad \text{(F-3)}$$

and thus

$$\bar{\epsilon} = \frac{-4c^2\left[c^2 + \frac{1}{2}(3d-2c)^2\right]}{3bd^3} \times 100. \qquad \text{(F-4)}$$

The errors were calculated for various values of d/b as a function of r/d from (F-2) and c/d from (F-4). These results are shown in Table 13.

APPENDIX G. COMPUTER ANALYSIS WORKSHEET

The tables in this report should suffice to permit error determinations. A computer program is available at MTL to expedite such computations however. MTL will compute the error analysis upon request if the following form is filled out as completely as possible and mailed to Mr. George Quinn.

Replies will be kept confidential.

Please use consistent units of measure, i.e., all dimensions in inches, millimeters, or centimeters, etc.

1.	Three- or four-point flexure: (circle one)	3 4
2.	Specimen height (thickness)	
3.	Specimen width	
4.	Specimen total length	
5.	Specimen edge chamfer radius or length* (circle one)	R L
6.	Fixture outer span	
7.	Fixture inner span (if 4-point)	
8.	Fixture outer bearing(s), radius	
9.	Fixture inner bearing(s), radius	
10.	Precision of the micrometer used to measure specimen height and width	
11.	Accuracy of the fixture spans	
12.	Specimen twist or lack of parallelism of two faces ⊕	
13.	Fixture twist ⊗ or lack of parallelism of bearings	
14.	Length of bearing fixture ○	
15.	Accuracy of centering the inner bearing(s) relative to the outer bearings	
16.	Do your fixture bearings rotate? Or are they fixed, such as knife edges? (circle one)	rotate fixed
17.	Do your fixture bearings articulate to accommodate specimen twist or warpage? (circle one)	yes no
18.	Error in measured break load	

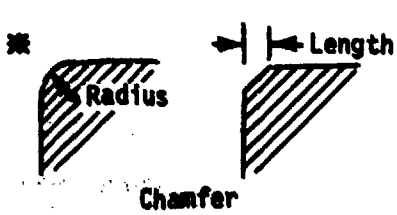

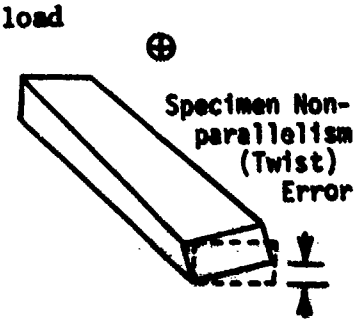

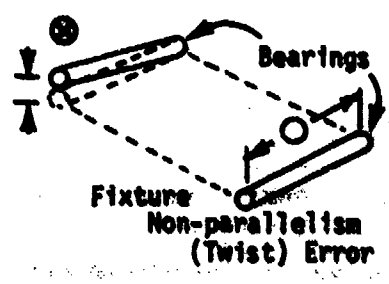

DISTRIBUTION LIST

No. of Copies	To
1	Office of the Under Secretary of Defense for Research and Engineering, The Pentagon, Washington, DC 20301
	Commander, U.S. Army Laboratory Command, 2800 Powder Mill Road, Adelphi, MD 20783-1145
1	ATTN: SLCIS-IM-TL
	Commander, Defense Technical Information Center, Cameron Station, Building 5, 5010 Duke Street, Alexandria, VA 22304-6145
2	ATTN: DTIC-FDAC
1	Metals and Ceramics Information Center, Battelle Columbus Laboratories, 505 King Avenue, Columbus, OH 43201
	Commander, Army Research Office, P.O. Box 12211, Research Triangle Park, NC 27709-2211
1	ATTN: Information Processing Office
	Commander, U.S. Army Materiel Command, 5001 Eisenhower Avenue, Alexandria, VA 22333
1	ATTN: AMCLD
	Commander, U.S. Army Materiel Systems Analysis Activity, Aberdeen Proving Ground, MD 21005
1	ATTN: AMXSY-MP, H. Cohen
	Commander, U.S. Army Electronics Research and Development Command, Fort Monmouth, NJ 07703
1	ATTN: AMDSD-L
1	AMDSD-E
	Commander, U.S. Army Missile Command, Redstone Scientific Information Center, Redstone Arsenal, AL 35898-5241
1	ATTN: AMSMI-RKP, J. Wright, Bldg. 7574
1	AMSMI-RD-CS-R, Documents
1	AMSMI-RLM
	Commander, U.S. Army Armament, Munitions and Chemical Command, Dover, NJ 07801
2	ATTN: Technical Library
1	AMDAR-QAC-E
1	AMDAR-LCA, Mr. Harry E. Pebly, Jr., PLASTEC, Director
	Commander, U.S. Army Natick Research, Development, and Engineering Center, Natick, MA 01760
1	ATTN: Technical Library
	Commander, U.S. Army Satellite Communications Agency, Fort Monmouth, NJ 07703
1	ATTN: Technical Document Center

No. of Copies	To
	Commander, U.S. Army Engineer School, Fort Belvoir, VA 22060
1	ATTN: Library
	Commander, U.S. Army Engineer Waterways Experiment Station, P. O. Box 631, Vicksburg, MS 39180
1	ATTN: Research Center Library
	Technical Director, Human Engineering Laboratories, Aberdeen Proving Ground, MD 21005
1	ATTN: Technical Reports Office
	Commandant, U.S. Army Quartermaster School, Fort Lee, VA 23801
1	ATTN: Quartermaster School Library
	Naval Research Laboratory, Washington, DC 20375
1	ATTN: Dr. C. I. Chang - Code 5830
2	Dr. G. R. Yoder - Code 6384
	Chief of Naval Research, Arlington, VA 22217
1	ATTN: Code 471
1	Edward J. Morrissey, AFWAL/MLTE, Wright-Patterson Air Force, Base, OH 45433
	Commander, U.S. Air Force Wright Aeronautical Laboratories, Wright-Patterson Air Force Base, OH 45433
1	ATTN: AFWAL/MLC
1	AFWAL/MLLP, M. Forney, Jr.
1	AFWAL/MLBC, Mr. Stanley Schulman
	National Aeronautics and Space Administration, Marshall Space Flight Center, Huntsville, AL 35812
1	ATTN: R. J. Schwinghammer, EH01, Dir, M&P Lab
1	Mr. W. A. Wilson, EH41, Bldg. 4612
	U.S. Department of Commerce, National Bureau of Standards, Gaithersburg, MD 20899
1	ATTN: Stephen M. Hsu, Chief, Ceramics Division, Institute for Materials Science and Engineering
1	Committee on Marine Structures, Marine Board, National Research Council, 2101 Constitution Ave., N.W., Washington, DC 20418
1	Librarian, Materials Sciences Corporation, Guynedd Plaza II, Bethlehem Pike, Spring House, PA 19477
1	The Charles Stark Draper Laboratory, 68 Albany Street, Cambridge, MA 02139
	Wyman-Gordon Company, Worcester, MA 01601
1	ATTN: Technical Library

No. of Copies	To
	Commander, U.S. Army Tank-Automotive Command, Warren, MI 48090
1	ATTN: AMSTA-ZSK
2	AMSTA-TSL, Technical Library
	Commander, White Sands Missile Range, NM 88002
1	ATTN: STEWS-WS-VT
	President, Airborne, Electronics and Special Warfare Board, Fort Bragg, NC 28307
1	ATTN: Library
	Director, U.S. Army Ballistic Research Laboratory, Aberdeen Proving Ground, MD 21005
1	ATTN: AMDAR-TSB-S (STINFO)
	Commander, Dugway Proving Ground, Dugway, UT 84022
1	ATTN: Technical Library, Technical Information Division
	Commander, Harry Diamond Laboratories, 2800 Powder Mill Road, Adelphi, MD 20783
1	ATTN: Technical Information Office
	Director, Benet Weapons Laboratory, LCWSL, USA AMCCOM, Watervliet, NY 12189
1	ATTN: AMSMC-LCB-TL
1	AMSMC-LCB-R
1	AMSMC-LCB-RM
1	AMSMC-LCB-RP
	Commander, U.S. Army Foreign Science and Technology Center, 220 7th Street, N.E., Charlottesville, VA 22901
1	ATTN: Military Tech
	Commander, U.S. Army Aeromedical Research Unit, P.O. Box 577, Fort Rucker, AL 36360
1	ATTN: Technical Library
	Director, Eustis Directorate, U.S. Army Air Mobility Research and Development Laboratory, Fort Eustis, VA 23604-5577
1	ATTN: SAVDL-E-MOS (AVSCOM)
	U.S. Army Aviation Training Library, Fort Rucker, AL 36360
1	ATTN: Building 5906-5907
	Commander, U.S. Army Agency for Aviation Safety, Fort Rucker, AL 36362
1	ATTN: Technical Library
	Commander, USACDC Air Defense Agency, Fort Bliss, TX 79916
1	ATTN: Technical Library

No. of Copies	To
	Lockheed-Georgia Company, 86 South Cobb Drive, Marietta, GA 30063
1	ATTN: Materials and Processes Engineering Dept. 71-11, Zone 54
	General Dynamics, Convair Aerospace Division, P.O. Box 748, Fort Worth, TX 76101
1	ATTN: Mfg. Engineering Technical Library
1	Mechanical Properties Data Center, Belfour Stulen Inc., 13917 W. Bay Shore Drive, Traverse City, MI 49684
1	Mr. R. J. Zentner, EAI Corporation, 198 Thomas Johnson Drive, Suite 16, Frederick, MD 21701
	Director, U.S. Army Materials Technology Laboratory, Watertown, MA 02172-0001
2	ATTN: SLCMT-IML
3	Authors

☆ U. S. GOVERNMENT PRINTING OFFICE: 1987--702-500--60106

U.S. Army Materials Technology Laboratory
Watertown, Massachusetts 02172-0001
ERRORS ASSOCIATED WITH FLEXURE TESTING
OF BRITTLE MATERIALS -
Francis I. Baratta, George D. Quinn,
and William T. Matthews

AD______________

UNCLASSIFIED
UNLIMITED DISTRIBUTION

Key Words

Flexural strength
Ceramic materials
Mechanical properties

Technical Report MTL TR 87-35, July 1987, 49 pp -
illus-tables

Requirements for accurate bend-testing of four-point and three-point beams of rectangular cross-section are outlined. The so-called simple beam theory assumptions are examined to yield beam geometry ratios that will result in minimum error when utilizing elasticity theory. Factors that give rise to additional errors when determining bend strength are examined, such as: wedging stress, contact stress, load mislocation, beam twisting, friction at beam contact points, contact point tangency shift, and neglect of corner radii or chamfer in the stress determination. Also included are the appropriate Weibull strength relationships and an estimate of errors in the determination of the Weibull parameters based on sample size. Such analyses and results provide guidance for the accurate determination of flexure strength of brittle materials within the linear elastic regime. Error tables resulting from these analyses are presented.

U.S. Army Materials Technology Laboratory
Watertown, Massachusetts 02172-0001
ERRORS ASSOCIATED WITH FLEXURE TESTING
OF BRITTLE MATERIALS -
Francis I. Baratta, George D. Quinn,
and William T. Matthews

AD______________

UNCLASSIFIED
UNLIMITED DISTRIBUTION

Key Words

Flexural strength
Ceramic materials
Mechanical properties

Technical Report MTL TR 87-35, July 1987, 49 pp -
illus-tables

Requirements for accurate bend-testing of four-point and three-point beams of rectangular cross-section are outlined. The so-called simple beam theory assumptions are examined to yield beam geometry ratios that will result in minimum error when utilizing elasticity theory. Factors that give rise to additional errors when determining bend strength are examined, such as: wedging stress, contact stress, load mislocation, beam twisting, friction at beam contact points, contact point tangency shift, and neglect of corner radii or chamfer in the stress determination. Also included are the appropriate Weibull strength relationships and an estimate of errors in the determination of the Weibull parameters based on sample size. Such analyses and results provide guidance for the accurate determination of flexure strength of brittle materials within the linear elastic regime. Error tables resulting from these analyses are presented.

U.S. Army Materials Technology Laboratory
Watertown, Massachusetts 02172-0001
ERRORS ASSOCIATED WITH FLEXURE TESTING
OF BRITTLE MATERIALS -
Francis I. Baratta, George D. Quinn,
and William T. Matthews

AD______________

UNCLASSIFIED
UNLIMITED DISTRIBUTION

Key Words

Flexural strength
Ceramic materials
Mechanical properties

Technical Report MTL TR 87-35, July 1987, 49 pp -
illus-tables

Requirements for accurate bend-testing of four-point and three-point beams of rectangular cross-section are outlined. The so-called simple beam theory assumptions are examined to yield beam geometry ratios that will result in minimum error when utilizing elasticity theory. Factors that give rise to additional errors when determining bend strength are examined, such as: wedging stress, contact stress, load mislocation, beam twisting, friction at beam contact points, contact point tangency shift, and neglect of corner radii or chamfer in the stress determination. Also included are the appropriate Weibull strength relationships and an estimate of errors in the determination of the Weibull parameters based on sample size. Such analyses and results provide guidance for the accurate determination of flexure strength of brittle materials within the linear elastic regime. Error tables resulting from these analyses are presented.

U.S. Army Materials Technology Laboratory
Watertown, Massachusetts 02172-0001
ERRORS ASSOCIATED WITH FLEXURE TESTING
OF BRITTLE MATERIALS -
Francis I. Baratta, George D. Quinn,
and William T. Matthews

AD______________

UNCLASSIFIED
UNLIMITED DISTRIBUTION

Key Words

Flexural strength
Ceramic materials
Mechanical properties

Technical Report MTL TR 87-35, July 1987, 49 pp -
illus-tables

Requirements for accurate bend-testing of four-point and three-point beams of rectangular cross-section are outlined. The so-called simple beam theory assumptions are examined to yield beam geometry ratios that will result in minimum error when utilizing elasticity theory. Factors that give rise to additional errors when determining bend strength are examined, such as: wedging stress, contact stress, load mislocation, beam twisting, friction at beam contact points, contact point tangency shift, and neglect of corner radii or chamfer in the stress determination. Also included are the appropriate Weibull strength relationships and an estimate of errors in the determination of the Weibull parameters based on sample size. Such analyses and results provide guidance for the accurate determination of flexure strength of brittle materials within the linear elastic regime. Error tables resulting from these analyses are presented.

SUPPLEMENTARY

INFORMATION

DEPARTMENT OF THE ARMY
U.S. ARMY LABORATORY COMMAND
MATERIALS TECHNOLOGY LABORATORY
WATERTOWN, MASSACHUSETTS 02172-0001

REPLY TO ATTENTION OF

AD-A187470

SLCMT-IMA-T

6 May 1988

MEMORANDUM FOR: SEE DISTRIBUTION

SUBJECT: Technical Report MTL TR 87-35, "Errors Associated with Flexure Testing of Brittle Materials"

Errata sheet for subject report:

Page 6, Table 4:

Change $E/\sigma_b = 500$ to $E/\sigma_b = 1000$.

Page 13, Equation 18a:

Add parentheses around $\sigma_b/2$ $(\sigma_b/2)$.

Page 14, Equation 18b:

Change the quantity (e/σ_b) to (E/σ_b).

Page 23, Table 14:

The second line from the bottom of the table; change ρ to P.

Page 37, Equation C-14:

Change the quantity $(b/\ell')^2$ to $(n/\ell')^2$.

Page 41, Equation F-1:

Change the quantity $\pi/16$ to $\pi/18$.

FOR THE COMMANDER:

Diane Valeri

~~1 Encl.~~
~~Dist List~~

DIANE VALERI
Chief
Publishing & Visual Information Br.